Oxo-Degradable Polyethylene Films

Jakub Kalus

Master Thesis
2007

Tomas Bata University in Zlín
Faculty of Technology

Univerzita Tomáše Bati ve Zlíně
Fakulta technologická
Ústav inženýrství polymerů
akademický rok: 2006/2007

ZADÁNÍ DIPLOMOVÉ PRÁCE

(PROJEKTU, UMĚLECKÉHO DÍLA, UMĚLECKÉHO VÝKONU)

Jméno a příjmení:	**Bc. Jakub KALUS**
Studijní program:	**N 2808 Chemie a technologie materiálů**
Studijní obor:	**Inženýrství polymerů**
Téma práce:	**Oxo-Degradable Polyethylene Films**

Zásady pro vypracování:

The work will focuse on a novel class of polymeric materials, so-called oxo-degradable polyethylene, intended for agricultural applications. The main attention will be paid to the interrelation between the durability and formulation of these systems. Two grades of polyethylene doped by various pro-degrading additives will be processed into films via extrusion blow moulding. Films will be exposed to UV light under the condition of accelerated ageing. Durability will be studied by both chemical analysis (spectroscopy analysis, carbonyl index determination) and viscoelastic and mechanical analysis to obtain the profound knowledge of the evolution in material properties upon the degradation process.

Rozsah práce:

Rozsah příloh:

Forma zpracování diplomové práce: **tištěná/elektronická**

Seznam odborné literatury:

Raff, RAV. Polyethylene. New York: Interscience Publishers, 1956.

Geuskens, G. Degradation and Stabilization of Polymers. London: Applied Science Publ., 1975.

Ehrenstein, GW. Polymeric Materials. Munich: Hanser, 2001.

Vedoucí diplomové práce:	**Ing. Roman Čermák, Ph.D.** Ústav inženýrství polymerů
Datum zadání diplomové práce:	**11. listopadu 2006**
Termín odevzdání diplomové práce:	**10. května 2007**

Ve Zlíně dne 5. února 2007

prof. Ing. Ignác Hoza, CSc.
děkan

UNIVERZITA TOMÁŠE BATI VE ZLÍNĚ
Fakulta technologická
L.S.
①

prof. Ing. Milan Mládek, CSc.
ředitel ústavu

ACKNOWLEDGEMENTS

This work is a result of three-month stay in Laboratoire de Photochimie Moléculaire et Macromoléculaire (CNRS, Clermont-Ferrand, France) supported by European Leonardo da Vinci programme and BECARIO association.

It was honour for me to cooperate with Groupe BARBIER, a French producer of investigated oxo-degradable mulching films.

I make reckoning of friendly approach of my supervisors prof. Sophie Commereuc and Roman Čermák, Ph.D. and of course all person, who were concerned in this research.

I thank to all.

I declare I worked on this Master thesis by myself and I have mentioned all the used literature.

Zlín, 25th April 2007 .....

Jakub Kalus

ABSTRACT

Oxo-biodegradation of blown polyethylene mulching films differed in the level of stabilizers, antioxidants and pro-oxidants has been studied. The degradation was followed by changes in infrared spectrum, dynamic viscosity and elongation at break during exposure of samples to the combination of ultraviolet light, heat, water and humidity. Different kinetics of degradation between photo-oxidation and thermo-oxidation was found. Significantly, water had an accelerating effect on the photo-oxidation of mulching films under study. In contrast, humid air during thermo-oxidation was found to be an inhibitor. Oxidised surface of the specimens was documented by stereomicroscopy.

Keywords: Polyethylene; Mulching film; Oxo-biodegradability; Pro-oxidant; Photo-oxidation; Thermo-oxidation; FTIR spectroscopy

RESUMÉ

Byla zkoumána oxo-biodegradabilita polyetylenových mulčovacích fólií lišících se v množství stabilizátorů, antioxidantů a prooxidantů. Degradace způsobená kombinovaným účinkem ultrafialového záření, tepla, vody a vlhkosti byla sledována pomocí změn v infračerveném spektru, dynamické viskozitě a prodloužení při přetržení. Byl potvrzen předpokládaný rozdíl v kinetice mezi fotooxidací a termooxidací. Dále bylo zjištěno, že voda silně urychlovala fotooxidaci zkoumaných mulčovacích fólií. Naproti tomu vlhký vzduch termooxidaci inhiboval. Zoxidovaný povrch vzorků byl doložen pomocí stereomikroskopie.

Klíčová slova: Polyetylen; Mulčovací fólie; Oxo-biodegradabilita; Prooxidant; Fotooxidace; Termooxidace; FTIR spektroskopie

TABLE OF CONTENT

INTRODUCTION

Nowadays, plastics cannot be seen as an inadequate replacement of the other materials. Plastics have become equivalent and they have extended those materials, which are wrongly called classical [1].

A convenient definition of plastic role is written in [2]: "Plastics are all around us today and help to make our personal lives cleaner, easier, safer, more convenient, and more enjoyable. Today, plastics increasingly provide an environmentally sound and cost-effective solution for many design challenges and technology breakthroughs. Think about the clothes we wear, the houses we live in, and how we travel. […] Whether we are shopping in a supermarket, having major surgery or merely brushing our teeth, plastics are an integral part of everything we do."

Moreover, plastics can be formed into an enormous variety of complex shapes and facilitate design solutions in thousands of applications. Of course, plastics have advantages too disadvantages that are well known. Nevertheless, they are irreplaceable today and the problems coupled with their existence must be solved.

Currently, most of commodity polymers are composed of relatively simple organic compounds consisted of carbon (C) and hydrogen (H) atoms [1]. Both are specifically low-density elements, which is expressed in low weight of plastics. This provides a number of advantages:

1. Less raw material consumed
2. Less energy in production
3. Easier handling/carrying
4. Less fuel in transport
5. Less air pollution in transport
6. Less waste

On the other hand, low specific weight of plastics combined with unfitting shape like films cause problems during waste disposal [3]. Plastic waste, as well as paper waste, contributes to the wind-blown debris in municipal solid waste[1] landfills. However, proper waste management techniques (i.e., covering wastes immediately after deposition) should limit the amount of this blowing debris.

Wastes are, surely, always the shady side. Evidently, it is the main purpose of inconsistent view on plastics; they represent significant part of the waste. Since plastics do not corrode or decompose with time [2], they provide durable and tough problem during waste disposal. While durability and weather resistance mean that they are ideal for long-life applications (which can last over fifty years in some cases), at the end of the products life the question "where with them" must be solved. There are just several possibilities [3]:

---

[1] Includes nonhazardous waste generated in households, commercial establishments, institutions, and light industrial wastes; it excludes industrial process wastes, agricultural wastes, mining wastes and sewage sludge [4].

1. Source reduction
2. Recycling[2]
3. Incineration[3] with energy recovery
4. Landfilling[4]

While source reduction and recycling as the preferred options might be a solution for everybody, landfilling and incineration are essential components of an integrated waste management system. Plastic recycling and the recovery of energy from plastic waste in Europe are growing at a rate of about 10 %/year [5,6]. Recycling growth rates for plastics have been fairly steady over the past 10 years. This represents 16 % of total plastic waste. Energy recovery is used in 31 % and landfills in the remaining 53 %.

However, not all the cases of life cycle of plastics are possible or advantageous to keep in control. This has led to the development of different types of self-degradable polymers [7]. Plastics of biological origin, which are produced from sustainable sources such as starch, are beginning to be used. However, the economics of producing these is still inconvenient and their production is more expensive than the production of pure polyolefins (PO) [8] apart from mechanical, physical and chemical properties that are evidently worse. Newly emerging oxo-degradable plastics based just on common PO might be smart solution for a lots of environmental problems [9]. Not only mass consumption of commodity products with short life cycle but also much of plastics in industry might be replaced with oxo-degradable plastics. One of such example is successful application of oxo-degradable polyethylene (PE) for mulching films (MF) in agriculture replacing normal MF, which always had to be removed after the growing season.

Thus, in this work, several types of MF are characterised with respect to mechanical, physical and chemical properties during several types of artificial weathering. The results serve not only as a Master thesis but also as a base for improved oxo-degradable film production in Group BARBIER, let us say the price to performance ratio. Significantly, not only economical but also huge ecological aspect in these materials must be seen and so importance of all the biodegradable plastics in general.

---

[2] A resource recovery method involving the collection and treatment of a waste product for use as raw material in the manufacture of the same or another product [4].

[3] A disposal method in which municipal solid waste is brought to a plant where it is burned either as received or after being processed to a more uniform fuel to generate steam or electricity [4].

[4] A method of solid waste disposal on a land [4].

1 THEORETICAL PART

1.1 Plasticulture

No technology has modified the course of horticultural crop production as the use of agricultural plastics [10]. While the automotive, construction and packaging industries are all seen as important growing markets for the plastic industry, the increasing use of plastics in agriculture is just impressive [11]. The term "plasticulture" has even been coined to define the use of plastics in agriculture.

Nowadays, the world consumption of plastic materials in agriculture amounts 6,500,000 tons annually [12]. About 500,000 hectares are under greenhouse and 4,500,000 hectares are under mulching films, globally [13]. Plastic irrigation systems cover more than 400,000 hectares worldwide, apart from silage bags, hay bale wraps and others. New developments in plastic additive technology are helping drive this forward. Significantly, special prodegrading additives (pro-degradants[5]) are used for decomposing of (agricultural) plastics at the end of life cycle.

Currently, plasticulture is a whole system approach to modifying microclimates in producing high quality and yielding horticultural products. In this section, the main areas of application of plastics in agriculture are described.

The history of plasticulture initiated in 1948, when professor Emery Myers Emmert at the University of Kentucky replaced more expensive glass as a greenhouse cover with PE [14]. In consequence, plasticulture was introduced up in Southern Europe, Japan and United States [15].

While in southern areas of Europe (Spain, Italy) greenhouse films are largely used, in North America primarily open field covered by MF are preferred [13]. In northern areas (Alaska) plasticulture is a method of warming soil to promote crop maturity and improve yields of many field-grown warm season crops [16].

Unfortunately, it is the common fact that the economic factor is key determinant. Crop production, using systems of plasticulture, is usually more expensive per unit of product than production without such systems during comparable periods of the year. These additional costs are usually justified if the monetary return per unit of product is higher. This occurs, if the product is of better quality, if overall production costs are compensated through better yields, or if crop production occurs when local cropping is impossible. Moreover, calculating the economic advantage is more complicated when imports from other producing areas are considered [15]. On the other hand, multiyear experience speaks for the benefit of plasticulture (see Fig. 1.1).

The control of the environment within a greenhouse may require large amounts of energy, making energy a prime factor in computing profitability. What did show promise was the

[5] Additives supporting degradation.

development of greenhouse to conserve energy. Moreover, covering a greenhouse with a double layer of PE to reduce the loss of heat energy is rated to be outstanding [17]. Inflating two layers of PE with air will reduce the loss of heat energy from a greenhouse by 40 % [18]. In different countries various materials are used. Whereas Japan uses mostly polyvinyl chloride (PVC), France and Italy found the equipment for the extrusion-blowing process of making PE much less capital intensive than the PVC equipment, and therefore they selected PE. On the other hand, PVC films have a better heat-retaining capacity than the others, but they are also more expensive.

Similarly, row covers or plastic low tunnels protect crops from frost, controls insects and viruses [19,20]. The lightweight and the permeability of present films allow gas exchange and penetration of rain and eliminate hand ventilation [21]. As already said, PVC film is still dominant in Asia, especially in Japan.

Large importance of plasticulture came with mulching films. However, because MF are the main goal of this work, it is described separately in the following capture.

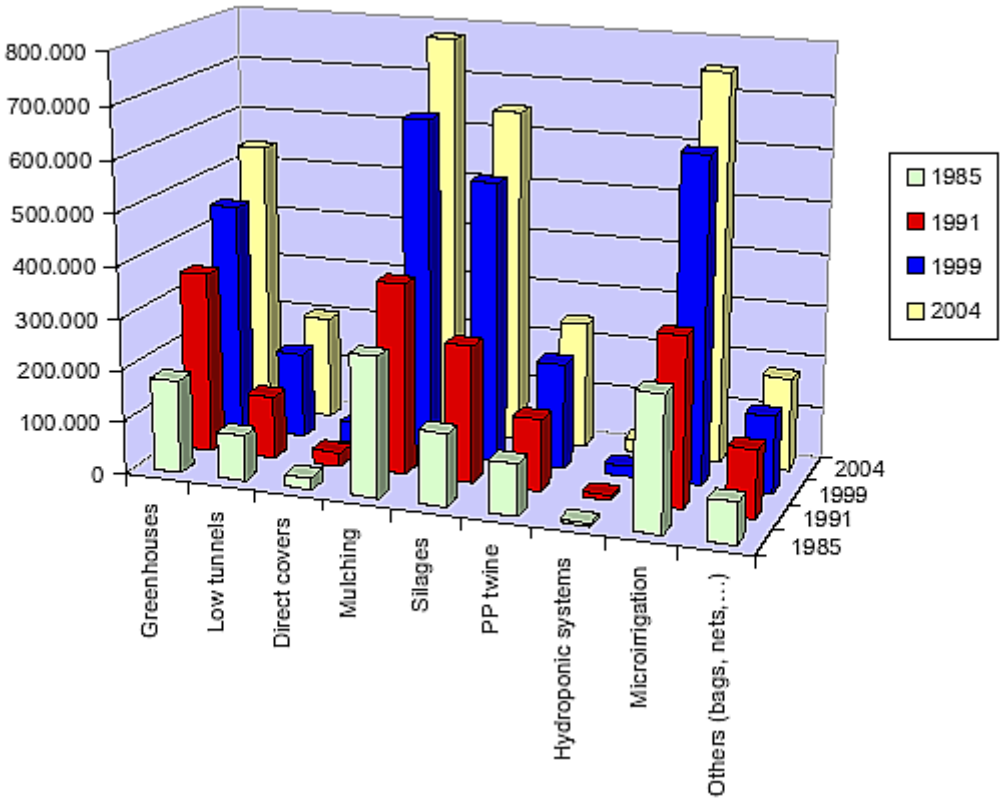

Fig. 1.1. *Quantities distribution (tons) of plastic products used in agriculture in the last two decades.*

1.2 Mulching films

Natural mulching films such as leaves, straw, sawdust, peat moss and compost have been used for centuries to control weeds, temperature and hold moisture and energy in the soil. However,

none of these materials have been employed to any greater extent in commercial vegetable production [22]. It is only in the last fifty years that synthetic materials have altered the methods and benefits of mulching.

Of historic MF such as paper, paper impregnated by wax, oil etc. only those made of PE are still used today in the agriculture. The preferred colours are transparent and black, although a wide variety of shades and colours are used for specific reasons in the production of food crops. Each colour has distinct optical characteristics and appears to affect plant growth and development [23,24]. Infrared transmitting (IRT) MF, which transmit most of the solar heat portion of light radiation but absorb most of the visible portion, were introduced to the market in the last decade [25]. IRT MF provide weed control as black MF does but increase the soil temperature, as with clear plastic MF. Significant advances in the use of MF occurred during the early 1960's with mechanization, when the mulch applicators and transplanters were invented which would plant directly through the MF.

A further economic advantage of plastic MF is economy in water and fertiliser usage. This is a major issue for the 21st century, since water will not be a plentiful commodity. Consequently, conservation will be necessary in order to produce crops in many dry climates of the world. It has been found that water usage during irrigation can be reduced by 80 % when it is released into the ground below a plastic cover [26]. In modern commercial agriculture, fertilisers are applied to the plants through the irrigation system and, due to the reduced water usage the use of fertilisers can also be reduced by 30 % compared with their usage on bare ground [27].

Usefulness of PE MF was also showed in northern climate, where they made possible to grow chilli, sweet potatoes forage maize and other crops [28]. Unfortunately, labour requirements to remove plastic MF from the field after the growing season can be high. In Taiwan, one of the most important market for MF, the cost of removing MF from the field before the next season is $250/hectare, irrespective of the value of the crops [29,30]. Moreover, only a small fraction of these plastics can be reused, due to damage, residues of earth and chemical products from plant treatments [31]. Oxo-degradable MF described in Capture 1.3 might be a solution.

1.3 Oxo-degradable mulching films

The use of degradable plastic films (e.g. PE) in tunnels and MF for the growing of soft fruits and vegetables has become an important economic tool in commercial agriculture and horticulture [32]. The first major use of degradable MF was in 1980’s [26]. After successful replacement of straw in strawberry and tomato growing, the application was introduced up in the USA and Italy, where it was employed for yielding production of melons [27,33]. Last but not least applications of degradable MF help to improve environment whether as scour protection, motorway embankments or as coal discarding because of self-degradability.

Several mechanisms of degradation of MF have been developed, but only those based on oxo-degradation of PE are important. Above all, it is necessary to get the degradation under control

by precise dosing of additives (antioxidants, stabilizers and pro-oxidants[6]) because the protective films must remain intact just before harvesting. Initially, MF create a microenvironment of the plant [27] so the prematurely degradation means the loss of benefits incomes. Furthermore, mechanical properties, especially elongation at break, must stay sufficient until the end of induction period (IP) and decrease quickly afterward [32].

Balanced addition of antioxidant, ultraviolet (UV) stabiliser and on the other hand pro-degradant is determining to achieve sufficient IP, but also rapid post-IP degradation. Surely, the supposed life cycle depends on the climes, so each type of oxo-degradable system must be set up with reasonable accuracy based on incident energy (mJ/m^2) and temperature. For this purpose, most of these time-controlled oxo-degradable plastics were developed in different companies and research centres so they are widely known under the brand name of the producer.

Significantly, it is necessary to discuss the influence of oxo-degradable MF especially pro-oxidants inside on the environment. Primarily, pro-oxidant transition metal ions (Fe, Mn, Co, Ni) required to initiate thermo- and photo-oxidation of the polyolefinic plastics are in huge publicity of "green" movements. No objective scientific study confirms the effects of "heavy metals" on plants and on humans or animals in consequence [34-37]. On the contrary, humans require the mentioned ions for normal metabolism and most of these are obtained from food plants, which in turn obtain them from the soil [32]. Anyway, if the same field was covered every year with Ni-containing MF it would take 500 years to increase the content of the topsoil by 1 ppm [33].

Experience with degradable MF has more recently led to the application of programmed-life polymers in other auxiliary products for agriculture. Moreover, commodity products with a short life cycle show to be an important target. New emerging materials based on oxo-degradable plastics reinforced by natural fibres so called eco-composites, seem to be the solution for many illness of present.

1.4 Oxo-degradation

Essentialy, no high molecular matter is normally biodegradable until it is degraded into low molecular mass species that can be assimilated by micro-organisms [38,39]. This means that the biodegradation process must be preceded by a biotic or abiotic degradation that gives monomeric or oligomeric products [40]. The final products of biodegradation are carbon dioxide, water, biomass and some residues.

Two main mechanisms have been recognized in the process of polymer bioassimilation. Firstly, hydro-biodegradation is the dominant process leading to hydrolysis of most of natural and some synthetic (heterochain) polymers (polysacharides, polyesters) [41-43]. In the case of hydrophobic

[6] Additives supporting oxo-degradation.

carbon backbone polymers (PH) especially PO, an analogous abiotic process, oxo-biodegradation can be employed [43-45].

The rate-determining part is an oxidation segment, commonly called peroxidation. It has been demonstrated [40-43,46-52] that the resulting biodegradation of oxidized molecular fragments from PO[7] occurs relatively rapidly. However, commercial PO undergo peroxidation quite slowly under the conditions in which they are normally employed and disposed. This is because of the presence of antioxidants and other stabilisers. Moreover, the rate and extent of the oxidation of PO are affected by structural parameters such as chain defects (unsaturation) or branching [53]. In this context it has been stated that the hierarchy in oxidation susceptibility of PO is following: iPP > LDPE > LLDPE > HDPE [54,55].

If the goal is to increase the sensitivity of PO to oxo-degradation, the peroxidation must be promoted by pro-oxidants [56]. The most active pro-oxidants are those based on metal combinations capable of yielding two metal ions of similar stability with oxidation number differing by one unit (M^n/M^{n+1}). Thus, the polymer degrades by a free radical ($^{\cdot}$) chain reaction involving oxygen (O_2) from the atmosphere (see Reacs. 1.1 – 1.4) [40]. Reacs. 1.1 - 1.4 lead to the rapid accumulation of polymer hydroperoxides (POOH) [32].

$$POOH + M^n \rightarrow PO^{\cdot} + OH^- + M^{n+1} \quad (1.1)$$

$$POOH + M^{n+1} \rightarrow POO^{\cdot} + H^+ + M^n \quad (1.2)$$

$$PO^{\cdot} + PH \rightarrow POH + P^{\cdot} \rightarrow POOH + P^{\cdot} \xrightarrow{O2+PH} P^{\cdot} + POOH \quad (1.3)$$

$$POO^{\cdot} + PH \rightarrow POOH + P^{\cdot} \xrightarrow{O2+PH} P^{\cdot} + POOH \quad (1.4)$$

The starting point is shown here as POOH, the formation of which resulted from shear stresses during extrusion, for example, that caused homolytic bond cleavage. The resultant carbon-centred radical reacted with the O_2 that is never removed completely from the system to form a peroxyl radical which, by hydrogen abstraction, is converted to a hydroperoxide group.

The primary products, polymer hydroperoxides, can either thermolyse or photolyse under the catalytic action of pro-oxidants (see Reacs. 1.1, 1.2) with chain scission and the production of low molecular mass oxidation products such as carboxylic acids, alcohols, ketones and low molecular mass hydrocarbon waxes [4,26,44,51,57-64] (see Fig. 1.2). One of the few differences between peroxidation initiated by heat and by light is that ketone products are stable to heat but not to UV light [65]. In either case, one is dealing with a branching chain reaction sequence in which the reaction of the hydroperoxide group is the rate-determining step in peroxidation leading up to molar mass reduction. Peroxidation leads also to hydrophilic surface modification. This is favourable to micro-organisms [41], which can then bioassimilate the low molecular mass oxidation products.

[7] All mechanisms and reactions considered for PO may be applied on PE.

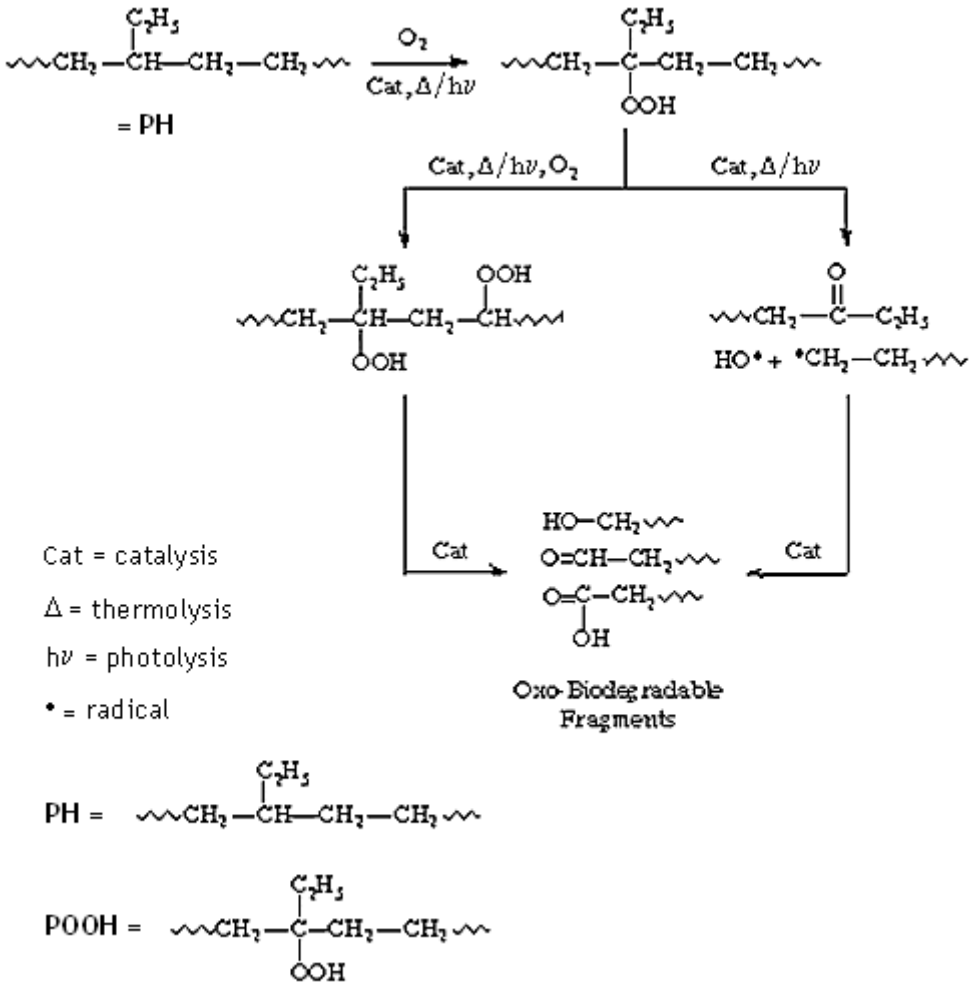

Fig. 1.2. *Mechanism of radical oxidation of PE*

The most deleterious part of total solar radiation is the UV radiation (wavelength region of 290 – 400 nm), which may be the most important factor in the photolysis in polymers used for outdoor purposes [66]. Although, pure PO are not expected to absorb UV radiation in this wavelength range. An efficient way to transfer the light energy into the polymer backbone is to make a copolymer with e.g. carbon monoxide, which acts as a chromophore [67-70]. Another way to make PE more sensitive to UV light is to incorporate photosensitizers, metal complexes, e.g. transition dithiocarbamates [57,71].

When the polymer is exposed to high temperature (i.e. heat accumulation on the field) the thermolysis of POOH occurs [72]. Generally, the influence of temperature is a critical factor in degradation as it can increase the rate of various chemical reactions [73].

However, polyolefinic MF must remain intact in the out-door environment for 3 months or more. Therefore, peroxidation must be controlled during the service life of the MF by peroxidolytic antioxidants that catalytically destroy surplus POOH. Consequently, they inhibit peroxidation until the antioxidants has been depleted by the action of light or heat [32].

The life cycle of oxo-degradable MF may be affected by different metal ions. While nickel, zinc and cobalt complexes act as stabilizers, iron and copper complexes act as sensitizers [74]. In the case of a combination of nickel dithiocarbamate (photo antioxidant) and iron dithiocarbamate (photo pro-oxidant) a wide range of embrittlement times is obtained in which the IP is controlled by the nickel complex and the post IP rate by the iron complex [75]. Iron dithiocarbamate at low concentrations causes very fast photodegradation of the polymer, but it shows a well-characterised IP, which increases with higher concentrations in the polymer [76]. Another important characteristic of this metal dithiocarbamate is that it also increases the stability of the PO to thermal oxidation during processing.

Finally in this chapter, it must be pointed out that the degradation of PO is a complicated process. The main degradation mechanism was explained but in most cases more than one mechanism takes place simultaneously during the life cycle of the products [77].

1.5 Polyethylene

Certainly, PE is the most frequently used polymeric material of daily consumption [78]. The high toughness, ductility, excellent chemical resistance, low water vapour permeability and very low water absorption, combined with the ease with which it can be processed, make PE an attractive choice for a variety of goods [79]. However, PE is limited by its relatively low modulus, yield stress and melting point.

The main reason for the wide use is simple structure together with wide variability of properties [1]. Rather than single polymer it looks like a whole group of polymeric materials that are construct of ethylene as a basic structural unit differing in the structure and number of units, branching, curing, chemical modification and last but not least, supermolecular structure. PE is quite often used as a material for morphological studies in polymer science, because of its illustration of the dependence between internal architecture and external properties [1,80].

Commercially, several distinct routes to the preparation of PE from ethylene are used [79]. Today, most of ethylene is obtained from petroleum sources. When supplies of natural or petroleum gas are available, the monomer is produced in high yield by high-temperature cracking of ethane and propane.

As the first (in March 1933 by R. Gibson and E. Fawcet [81]) low-density PE (LDPE) was prepared by polymerisation of ethylene under high pressure (100 - 300 MPa). This method gives polymer molecules that are branched to varying extents and of moderate number average molecular weight, generally less than 50,000. However, in 1954 two other routes were developed, first using metal oxide catalysts (e.g. the Phillips process) and the second using aluminium alkyl or similar materials (the Ziegler process) [82]. By these processes polymers could be prepared at lower temperatures and pressures and with a modified structure [79]. Because of these modifications, both LDPE and high-density PE (HDPE) have different structures and properties. Due to side branches caused by more frequent transfer during polymerisation, the chains inside

LDPE supermolecular structure are not as well organized as in linear HDPE. As a result, LDPE has lower modulus, hardness and melting temperature. On the other hand, thanks to the lower crystallinity the transparency is higher.

At the end of the 1970s considerable interest was raised by linear low-density PE (LLDPE), which is intermediate in properties and structure to the high- and low-pressure produced materials. The short branches on the chain are produced by including small amounts of propene, but-1-ene, hex-1-ene or oct-1-ene into the monomer charge. Consequently, LLDPE is rather copolymer. Usage of LLDPE is now of the same order as of the other two materials.

With respect to chemical structure and properties, the basic chemical formula of PE is repeated structure $(-CH_2CH_2-)_n$, where n typically is in the range of 10^3-10^6. In ideal thermodynamic form (the lowest potential energy) PE occupies the planar zigzag conformation [83] (see Fig. 1.3).

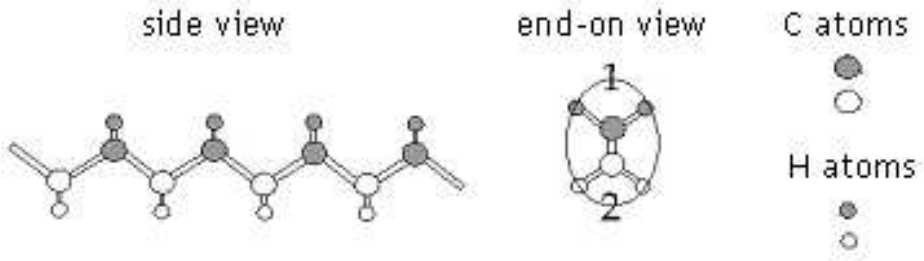

***Fig. 1.3**. The all trans conformation (zigzag) of PE. Side- and end-on view. The ellipse is drawn to facilitate the display of PE crystalline forms.*

Normally, PE crystallises in the orthorhombic crystalline form (Fig. 1.4, A) [84]. The orthorhombic PE crystalline unit cell has the following dimensions: a = 0.74 nm, b = 0.494 nm and c = 0.2534 nm. It was found that under extreme conditions, for example crystallisation with extreme cooling rates or crystallisation under stress, PE could crystallised also in the monoclinic form (Fig. 1.4, B). The monoclinic PE crystalline unit cell has the following cell dimensions: a = 0.809 nm, b = 0.253 nm and c = 0.479 nm.

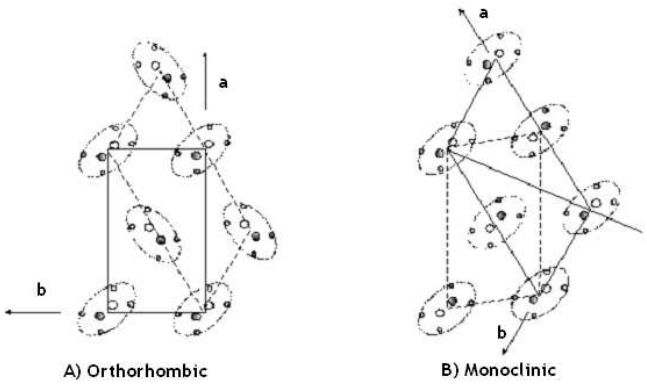

***Fig. 1.4**. Orthorhombic and monoclinic crystalline forms of PE. Cut through ab - plane with macromolecular long axes perpendicular to it.*

Some data on thermodynamic and mechanic properties of PE are summarised in Table 1.1.

Table 1.1*. Thermodynamic and mechanical properties of PE.*

Property		Value
Melting point	[°C]	~138
Glass transition temperature	[°C]	-128 – (-30)
Elongation at break	[%]	20 – 800
Tensile strength	[Mpa]	22 – 27.5
E-modulus	[Mpa]	700 – 1400
Izod impact strength	[J]	2 – 6.8

PE is an aliphatic hydrocarbon polymer with thermoplastic properties. However, in some conditions it can be cured by radiation, peroxides or by vinyl silane [79]. Cross-linked PE is being used for applications where service temperatures up to 90 °C are encountered.

After their discovery, polyethylenic materials were rapidly accepted by industry particularly in the manufacture of film [79]. By the mid-1990s the capacity for PE production was about 50,000,000 tons/year, much greater than for any other type of plastic material. Of this capacity about 40 % was for HDPE, 36 % for LDPE and about 24 % for LLDPE. Significantly, some 5 % of the PE produced is used for agricultural film applications.

1.6 FTIR analysis

Infrared (IR) and Raman spectroscopies are rapid and relatively inexpensive techniques providing qualitative and quantitative information of IR-active molecules in organic or inorganic solid, liquid or gas samples [85,86]. Both methods cause molecules to undergo in vibrational energy state by subjecting them to excitation in selected spectral regions.

Three main effects of interaction between matter and photon are common [87]:

1. reflection
2. transmission
3. absorption

In consequence, the principle of spectroscopy is registration of absorption (absorbance) or transmission (transmittance). In dependence on wavelength/frequency (energy) of the source, IR, UV and visible spectroscopy are mostly distinguished.

In any case, absorption band can be characterised by two parameters: the wavelength at which maximum absorbance occurs (qualitative analysis) and the intensity of the band, which is proportional to the number of molecules observed (quantitative analysis).

The transmittance can be calculated according to Eq. 1.1. The transmission spectrum is then obtained by plotting the transmittance versus the wavenumber. Similarly, the absorbance can be

obtained by using the Lambert-Beer equation (Eq. 1.2). A plot of absorbance versus wavenumber yields an absorption spectrum.

$$T = \frac{\Phi}{\Phi_0} \tag{1.1}$$

$$A = \log\left(\frac{\Phi_0}{\Phi}\right) = \varepsilon_\lambda c_M l \tag{1.2}$$

where T is transmittance, A is absorbance, Φ_0 is intensity of entering radiation (before sample absorption), Φ is intensity of transmitted radiation (after sample absorption), ε_λ is absorptivity [$dm^3mol^{-1}cm^{-1}$], c_M is molar concentration [mol dm^{-3}] and l is cell thickness [cm].

In IR spectroscopy, the vibrational excitation is achieved by radiating the sample with a broad-band source of radiation in the IR region, which is generally 4000-200 cm^{-1} (2.5-50 μm)[8] [85]. Each molecule has certain natural vibrational frequencies [88]. When IR light is incident on the molecule, the frequency that matches the natural vibrational frequency is absorbed by the molecule resulting in molecular vibrations. Consequently, a change in dipole moment of the molecule occurs. As illustrated in Fig. 1.5, the molecule is excited to a higher vibrational state by directly absorbing the IR radiation.

The implementation of Fourier transformation caused revolution in spectroscopy [85]. The main component in the Fourier Transform Infrared (FTIR) spectrometer is an interferometer [88]. This device splits and recombines a beam of light resulting in a wavelength-dependent interference pattern or an interferogram. The Michelson interferometer is most commonly used [89]. It consists of two mirrors and a beamsplitter positioned at an angle of 45° to the mirrors. IR radiation is projected onto the beamsplitter [90]. An ideal beamsplitter consists of a non-absorbing film, which transmits 50 % of the radiation to the mirror which is moving back and forth at a constant speed, whereas 50 % of the radiation is reflected to the fixed mirror. After being reflected, the two beams will recombine at the beamsplitter where interference between the beams takes place.

With polychromatic light (radiation with more than a single wavelength), the output signal is the sum of the entire cosine waves, which is the interferogram generated by constructive and destructive interference of the light. The interferogram contains the basic information on frequencies and intensities characteristic of a spectrum but in a form that is not directly interpretable. Thus, the information is converted to a more familiar form, a spectrum, using Fourier Transform methods.

---

[8] The wavenumber $\overline{\nu}$ [cm^{-1}] is the number of waves/centimeter. It is equal to the reciprocal of the wavelength λ [cm] and is equal to frequency ν [s^{-1} or Hz] divided by c, the velocity of light [cm s^{-1}]. In the IR region, the wavelength λ is given in micrometers μm or 10^{-6} m.

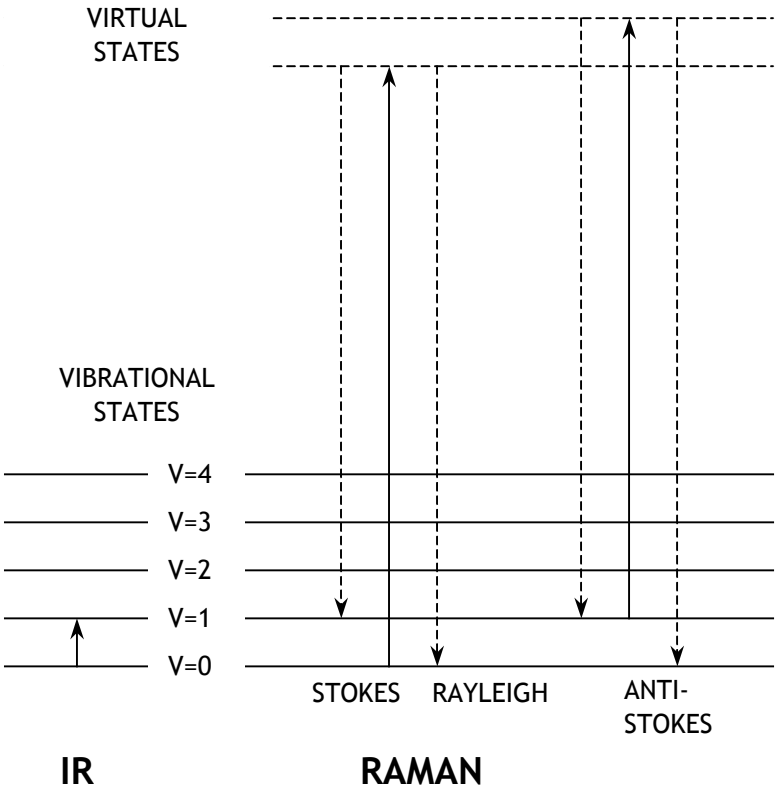

***Fig. 1.5**. Energy states involved in IR and Raman spectroscopies.*

Mathematically, the signal treatment can be described in the following way: If I(x) is the intensity of the beam measured at the detector at a displacement of the movable mirror by x cm and if B(ν) represents the intensity of the source as a function of ν, the equation for the signal at the detector (i.e. the interferogram) can be written:

$$I(x) = B(\nu)\cos 2\pi\nu x \tag{1.3}$$

For a dichromatic source (with frequencies ν_1 and ν_2), the signal at the detector is the sum of two cosine waves:

$$I(x) = B(\nu_1)\cos 2\pi\nu_1 x + B(\nu_2)\cos 2\pi\nu_2 x \tag{1.4}$$

For a polychromatic source, as in a real instrument, the detector signal or the interferogram is related to the spectrum by:

$$I(x) = \frac{1}{2\pi}\int_{-\infty}^{+\infty} B(\nu)\cos 2\pi\nu x d\nu \tag{1.5}$$

The spectrum is related to the interferogram by the following:

$$B(\nu) = \int_{-\infty}^{+\infty} I(x)\cos 2\pi\nu x d\nu \tag{1.6}$$

where I(x) is intensity at the detector, B(ν) is intensity of the source, ν is frequency [s^{-1}] and x is mirror displacement [m].

Eqs. 1.5 and 1.6 relate an interferogram to an IR singlebeam spectrum via the mathematics of the Fourier transform. The signal described by Eq. 1.5 is more or less constant during the mirror scan, but when the mirrors are equidistant from the beamsplitter, all waves are in phase and the interferogram shows a so-called centre burst.

Transmission type of IR spectroscopy is typically carried out in the laboratory [86]. The basic components of transmission FTIR spectroscopy are the spectrometer, data station and device for data output. Nowadays, proper software and FTIR spectrum library for evaluation of spectrum are essential.

1.7 Rheological properties

Rheometry is an extremely useful branch of continuum mechanics. The term rheology was originally defined on April 29, 1929 by a committee that met in Columbus, Ohio, after a proposal by E. C. Bingham and M. Reiner. By definition, the term refers to “the study of the deformation and flow of matter” [91-93] in terms of stress, strain, temperature and time, i.e. it is concerned with the description of the flow behaviour of all types of mater [94]. The term was inspired by Heraclitus's famous expression “panta rei”, “everything flows”.

Preliminary imagine a small deformable cube of an ideal solid material [95-98]. Suppose a force (F [N]) applied to the upper plane of the x-axis of the cube (see Fig. 1.6). The vertical edge is moved through an angle (α) and a net stretch on the cube is generated as a consequence of the force. The relative deformation of the cube is termed (shear) strain (γ).

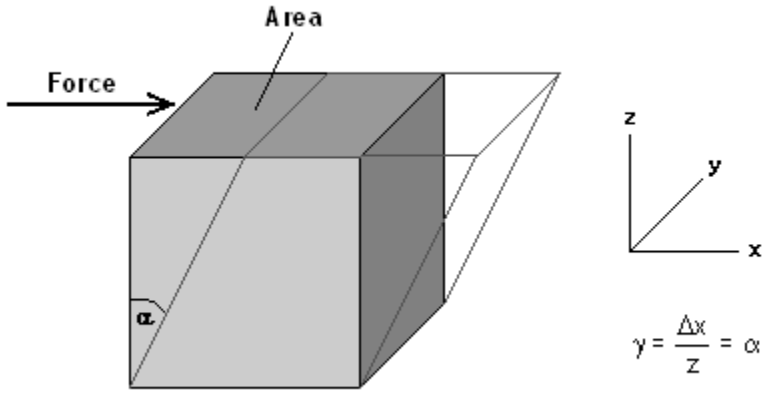

***Fig. 1.6**. The shear stress and shear strain on a cube.*

Dependence of the force on area (A [m^2]) of the cube on which it acts is solved by (shear) stress (σ [$N.m^{-2}$ = Pa]) defined as the force divided by the area of the face of the cube (σ = F/A). A

fundamental property of a material, the shear modulus (G [Pa]), is given as the stress divided by the strain ($G = \sigma/\gamma$). For a material that acts as a linear, G maintains a constant value regardless of stress or strain applied. Such material is called a Hookean solid.

Because many materials have essentially fluid behaviours so it is difficult to practically arrange a simple cube, imagine an element of ideal fluid between two parallel planar walls (see Fig. 1.7).

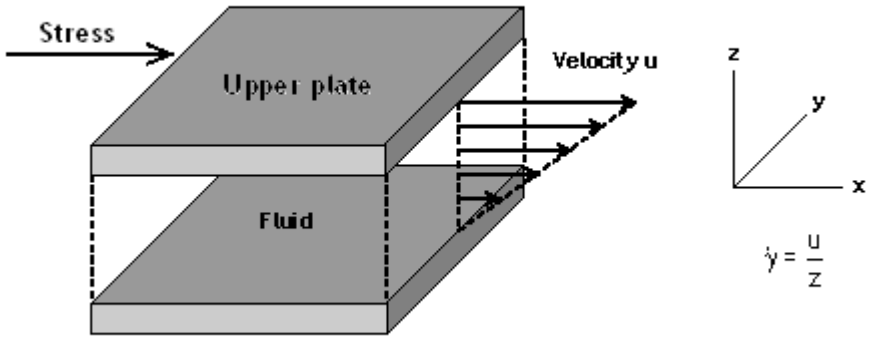

Fig. 1.7*. The shear stress and shear rate on two plates.*

Suppose a stress applied to the upper surface whilst maintaining the lower surface static, a velocity gradient will develop with the distance z across the gap. As the material is liquid, the displacement in the x direction is continuous. The strain provides the linear change of a velocity and increases constantly with time (Eq. 1.7).

$$\dot{\gamma} = \frac{d\gamma(t)}{dt} = \frac{1}{z}\frac{dx}{dt} = \frac{u}{z} \tag{1.7}$$

$\dot{\gamma}$ [s^{-1}] is the strain rate in time for a constant applied velocity invariant with the time. The most important relationship between σ and $\dot{\gamma}$ is defined by Eq. 1.8. Such equation defines fundamental property of each material, (shear) viscosity (η [Pas]).

$$\eta = \frac{\sigma}{\dot{\gamma}} \tag{1.8}$$

A material, which maintains the constant η regardless of the σ or $\dot{\gamma}$ applied is described as linear or Newtonian. The fluids in which the energy is stored are called non-Newtonian.

Let approximate non-Newtonian behaviour. If a γ is imposed on a solid sample by the application of a σ, the size of the σ is determined by the G. If there is a little fluid character to solid and if the molecules that form the material begin to rearrange and move relative to each other, the energy stored in the structure is dissipated by the flow and the σ begins to reduce. The balance of elastic and viscous processes determines the rate at which the sample relaxes. Consequently, a relaxation time (τ [s]) is defined as the ratio of the η to the G (Eq. 1.9).

$$\tau = \frac{\eta}{G} \tag{1.9}$$

Material loading at times shorter than τ shows elastic character and at longer times viscous character. A ratio of the τ to the experimental observation time (t [s]) can be defined by Eq. 1.10. Deborah number (De) is explained as a tendency of material to appear either viscous or elastic.

$$De = \frac{\tau}{t} \tag{1.10}$$

Material with De >> 1 is classified as a solid. If De << 1, liquid character appears. However, there are some materials like polymer viscous and elastic together. The De ~ 1 and therefore are called viscoelastic [1].

Several phenomenal properties are the symptom of viscoelastic behaviour [99,100]. Primary, the fluid rate inside a pipe does not increase linearly with an applied pressure drop, which is called non-linear flow. Another phenomenon is a dramatic resistance to stretching of fluid elements, the extensional viscosity. It is resistance of the fluid to stretching motions.

Storing of energy is typical symptom of non-Newtonian fluids. By this viscoelastic behaviour die swell and siphon effect come. The final category of non-Newtonian behaviour is normal stress effects. This effect can be viewed as being due to tension in the streamlines of the flow. Hence, fluid climbing up the axis of a mixer may be explained.

There are several ways to measure rheological properties of polymer melts. The simplest one, plate – plate rheometer, as a matter of fact, was explained in Fig. 1.7. The liquid lies between two parallel plates with the top plate free to move under an applied force and the bottom plate held fixed.

Rheometer with the parallel-plate geometry quite often carries out small amplitude oscillatory shear tests [101,102]. These tests involve the application of a sinusoidal stress (or strain) to the upper plate of the rheometer. The resulting strain (or stress) can be resolved into components that are in phase with the input (elastic response) and $\pi/2$ out of phase with the input (viscous response). Different complex functions are generally available for oscillatory experiment expression [103]. Collective connexion of complex modulus (G*) and complex viscosity (η^*) is showed by Eqs. 1.11 [104].

$$G^*(\omega) = G'(\omega) + iG''(\omega) \rightarrow \eta^*(\omega) = \eta'(\omega) - i\eta''(\omega) = G^*/i\omega \tag{1.11}$$

where G' and η' are storage magnitudes, G'' and η'' are loss magnitudes, ω is angular frequency [rad s^{-1}] and i is the imaginary unit.

Viscoelastic character of polymer melts in stress to strain shift appears, which is expressed by the loss angle (δ) defined by Eq. 1.12.

$$\tan\delta = \frac{G''}{G'} = \frac{\eta'}{\eta''} \tag{1.12}$$

On the basis of rheological experiments molecular weight may be determined. It is well known that the zero shear viscosity (η_0) depends on the molecular weight (M_w) and obeys a power law (Eq. 1.13) [105].

$$\eta_0 \propto M_w^{\alpha} \tag{1.13}$$

The exponent α is invariable. For supercritical molecular weight (typically for all common polymers) α = 3.4. The zero shear viscosity can be obtained from the η^* (Eq. 1.14) extrapolated to zero ω (Eq. 1.15) [106].

$$\eta^* = \frac{G^*(\omega)}{i\omega} = \eta' - i\eta'' \tag{1.14}$$

$$\left|\eta^*\right|_{\omega\to 0} = \eta_0 \tag{1.15}$$

Both, η' and η'' components of the η^* that are carried out to a diagram $\eta'' = (\eta'')\eta'$ seem to be located on the arc of a circle [104]. Let suppose fit circle smoothing the data. The centre of the circle situated below the η' axis is known. On the basis of η^* definition [101] the exact expressions of η_0 may be determined using Cole-Cole distribution (Eqs. 1.16) [107,108].

$$\eta^*(\omega) = \frac{\eta_0}{1 + (i\omega\lambda_0)^{1-h}} \tag{1.16}$$

where λ_0 is average relaxation time [s] and h is parameter of relaxation time distribution.

1.8 Mechanical properties

Uniaxial tensile testing is the most convenient way to study the mechanical properties of polymeric materials [109]. Tensile tests are simple, relatively inexpensive and fully standardized [110]. Data from test are used to determine elastic limit, elongation, modulus of elasticity, proportional limit, reduction in area, tensile strength, yield point and other tensile properties.

In principle, the tensile test applies an axial strain to a standard specimen and measurements are taken of the change in length between two specified marks, defined as the gauge length and also of the resulting tensile load [109,110]. Alternatively, the test could be carried out by applying a dead load and recording the subsequent strain on tensile testing machine.

Fig. 1.8 shows typical dumbbell specimen for tensile test with original cross-sectional area. The specimen should be broken in 60 seconds. Because of non-linear viscoelastic behaviour of the polymeric materials, the specimen geometry, deformation rate, temperature and humidity are essential to regular interpretation of tensile results.

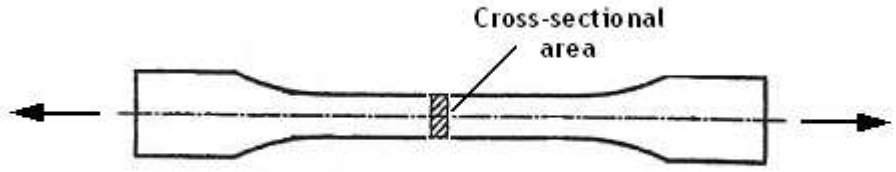

***Fig. 1.8**. Tensile dumbbell specimen.*

When stress is applied to a solid, strain (ε [%], let use ε for tensile testing) results [109]. This represents specific stress-strain diagram for each material. The diagram in Fig. 1.9 is characterised by lower and upper yield point, which is typical for drawable plastics.

Several most significant points (a – g) in tensile diagram (Fig. 1.8) can be distinguished [109-111]. Each point in the diagram is characterised by corresponding ε and σ.

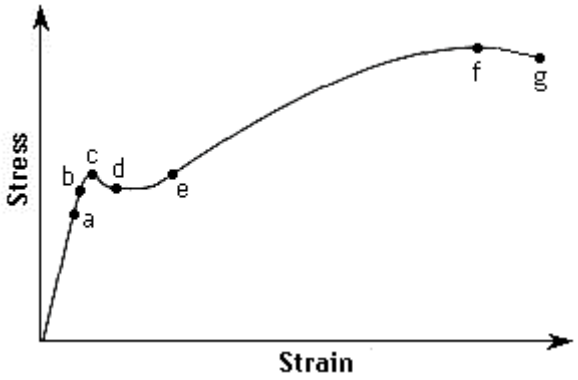

***Fig. 1.9**. Characteristic points of the tensile diagram.*

Proportional limit (point a) is the highest stress at which stress is directly proportional to strain. Up to this point the material obeys Hooke's law (Eq. 1.17).

$$\sigma = E\varepsilon \tag{1.17}$$

where E [Pa] is modulus of elasticity (Young's Modulus) and ε is defined as the elongation (ΔL [m]) per length (L [m]).

For the instantaneous true ε increment dε is done by Eq. 1.18.

$$d\varepsilon = \frac{dL}{L} \tag{1.18}$$

and after integration

$$\int_0^{\varepsilon} d\varepsilon = \int_{L_0}^{L_0+\Delta L} \frac{dL}{L} \tag{1.19}$$

ε is done by Eq. (1.20).

$$\varepsilon = \ln\left(\frac{L_0 + \Delta L}{L_0}\right) = \ln\left(1 + \frac{\Delta L}{L_0}\right) \tag{1.20}$$

For strain of about 1 %, the error in using the engineering strain versus the true strain is of order of 10^{-4}, so Eq. 1.6 may be written as Eq. 1.21.

$$\varepsilon = \frac{\Delta L}{L_0} \tag{1.21}$$

where L_0 is initial length [m].

The modulus of elasticity is a measure of the stiffness of the material, but it only applies in the linear region of the curve, so the slope is proportional to tangent modulus at origin. If a specimen is loaded within this linear region, the material will return to its exact same condition if the load is removed, so in this region of diagram elastic deformation occurs.

Loading up to *elastic limit point* (point b) is reversible and the unloading curve retraces the loading curve. In practice the elastic limit occurs just after the limit of proportionality. After this point any unloading curve is usually a straight line parallel to the elastic line.

Because taking the elastic limit is difficult, more often contract elastic limit is used. It is a stress, which permanent deformation, for example 0.1 % of original length induces.

Upper yield point (point c) in stress-strain diagram of a material is defined as the stress applied to the material at which plastic deformation starts to occur while the material is loaded. The upper yield point is often defined as the stress that gives rise to a 0.2 % permanent plastic strain. However, there may be the *lower yield point* (point d) that comes after upper yield point.

If the test is carried out by applying a load rather than an extension then the extension will increase from point c without any increase in load to the point e.

One of the properties describing a material is its *ultimate tensile strength* (UTS) (point f). This is the maximum load the specimen sustains during the test. The UTS may or may not equate to the strength at break. This all depends on the type of material like brittle, ductile, or a substance that even exhibits both properties.

The course between e and f point is quite distinct for each group of materials. For example, ultimate elongation values of several hundred percent are common for elastomers and PO. On the other hand, rigid plastics often exhibit values under 5 %.

After UTS will form in the specimen a large reduction in the cross-section area until failure occurs at point g called *strength at break*.

The deformation process is terminated by fracture. In a brittle material this occurs by the propagation of cracks initiated at the microscopic flaws in the material. Cracks propagate by cleavage, which involves breaking of atomic bonds along specific crystallographic planes, with the work of fracture spent primarily on creating a new surface (i.e., surface energy). On the

other hand, ductile materials tend to fail by nucleation of microvoids at second phase particles, and the subsequent growth and coalescence of these microvoids.

The tensile testing machine consists of a test frame with a fixed beam, a moving beam and a drive [111]. The specimen is mounted between two grips, one attached to the fixed beam and the other attached to the crosshead beam. The crosshead contains a load cell, which measures the tensile force on the specimen. The movement of the crosshead relative to the fixed beam generates strain within the specimen and a corresponding load.

During a tension test, it is desirable to apply force to the specimen large enough to break it. The grip region of the specimen must have a large enough area to transmit the force without significant deformation or slipping. While most material properties are supposed to be specimen geometry and grip independent, there are some weak dependencies. Consequently, standards also prescribe the whole test methods so that data may be reported in a very standardized way [112-114].

2 EXPERIMENTAL PART

Used material, techniques of degradation, evaluation of degradation and instruments are described in this section.

2.1 Material

Oxo-degradability of eight types of MF (DCST, DC89, DGUV, 10PD, DCRG, GDTP, DC55 and DCN82) supplied by Groupe BARBIER (Sainte Sigolene, France) was investigated. Extrusion blowing line was used for production of these films with average thickness about 10 μm. LDPE or both LDPE and LLDPE combined with a common additives were included into a base compound.

To ensure oxo-degradability pro-oxidants to the compound were added. On the basis of application of individual film and longtime experiences of the company a proper composition is chosen. However, the information of the certain film composition is confidential.

2.2 Preparation of specimens

The preparation of specimens from MF depended on subsequent evaluation of degradation. For FTIR analysis, the films were fixed between small rectangular aluminium plates (10 mm × 60 mm) with an aperture in the middle. For stereomicroscopy, rheological properties and mechanical properties the films were fixed between bigger aluminium plates (50 mm × 100 mm with aperture 30 mm × 70 mm) and placed in SEPAP 12/24.

Different system of fixation of films was used for thermal degradation that was evaluated by rheology or tensile testing. To ensure sufficient access of air the specimens were hanged on a screen and placed into the oven.

2.3 Techniques of degradation

Several techniques of artificial and natural ageing of MF were studied. Following basic processes may be distinguished which may appear in individual techniques of degradation: UV light, heat, water and humidity.

2.3.1 Photo oxo-degradation

For photo oxo-degradation (artificial weathering) SEPAP 12/24 (MPC L8) developed by the Laboratoire de Photochimie Moléculaire et Macromoléculaire (Clermont-Ferrand, France) was used [115]. Four mercury vapour arc lamps (Novalamp, 400W) with a borosilicate envelop

supplied radiation in the wavelength range between 290 and 450 nm. Each lamp was located in one corner of a test chamber. Specimens turned with a carousel holder in the middle.

A Pt 1000 temperature sensor connected with a microprocessor temperature regulator device, which controls a fan, measured temperature of the specimens. All the experiments were carried out at 60 ± 2 °C. Photo oxo-degraded specimens were analysed by FTIR spectroscopy, rheological and mechanical properties.

2.3.2 Natural ageing

A relationship between natural ageing and artificial ageing is solved quite often. To secure approximate comparison the most oxo-degradable specimens (DC89 and DC55) were placed on the frame directed angle-wise 45° to southern sky.

FTIR spectrum after outdoor exposure was measured and from the absorbance in carbonyl band corresponding time for artificial ageing in SEPAP 12/24 was evaluated.

2.3.3 Thermo oxo-degradation

Other important factor, responsible for thermo oxo-degradation, is heat. Thermal degradation of all the films was carried out in free convection laboratory oven (Memmert) at 60 °C, under dry conditions[9] (uncontrolled humidity). To ensure comparability the same techniques of evaluation of degradation like by photo oxo-degradation were applied.

2.3.4 Thermo oxo-degradation with controlled humidity

Retention of water as a moisture is significant part of MF so influence of humidity was studied. The thermo oxo-degradation with controlled humidity was simulated in oven with 70 % of relative humidity at 80 °C (VC 4034 Vötsch Industrietechnik). The degradation was evaluated by FTIR spectroscopy.

2.3.5 Effect of water

Sharing of matter is an important factor of each transient process. By diffusion of prodegrading additives from MF into the water or some chemical modification the rate of degradation might be affected. For this purpose, effect of water was also studied.

Two groups of specimens (DCST, DC89, GDTP and DC55) bathed inside two close glass tanks with about 300 ml of distilled water (ambient temperature approx. 20 °C and 60 °C in the oven) for 16 days (in the dark). The water was replaced every two days. After exposure in the water and

[9] No device for measuring of RH at 60 °C was available. The RH at ambient temperature (23 °C) was around 30 %, which means that RH at 60 °C was about 5 %.

careful drying of specimens the photo degradation in SEPAP 12/24 at 60 °C proceeded. FTIR spectroscopy was used for determination of degradation.

2.4 Evaluation of degradation

2.4.1 FTIR spectroscopy

Transmission FTIR spectroscopy analysis (Nicolet, Impact 400) was applied to determine chemical changes of the macromolecule. The whole mid-infrared spectrum (4000 – 500 cm^{-1}) was measured. The spectra were taken as an average of 32 scans with 2 cm^{-1} resolution.

Carbonyl peak increase as a consequence of photo oxo-degradation, thermo oxo-degradation and natural weathering was observed and its height (absorbance) in approx. 1715 cm^{-1} (1712 – 1716 cm^{-1}, region of carboxylic acid group absorbance) evaluated (Omnic® software).

For collective comparison of absorbance of carbonyl band and degradability in consequence, the thickness normalizing was done. The thickness of each specimen before degrading was measured (M120, Messmer Instruments Ltd.) and average and standard deviation from 10 measurements evaluated. For normalizing Eq. 2.1 was applied.

$$A_C = \frac{t_{S0}}{t_0} A \tag{2.1}$$

where A_C is corrected absorbance of existent specimen, A is measured absorbance of existent specimen, t_{S0} is thickness of standard specimen before degradation and t_0 is thickness of existent specimen before degradation. The DCST was always chosen as a standard.

For qualification as a photo oxo-degradable material after degradation in SEPAP 12/24 at 60 °C Eq. 2.2 must be satisfied (Critère 2 [116]).

$$A_{100} = \frac{A_0}{100} \pm 20\% \tag{2.2}$$

where A_{100} is absorbance after 100-hour exposure without IP and A_0 is absorb. before exposure.

For qualification as a thermo oxo-degradable material after degradation in the oven at 60 °C condition of the IP between 400 and 1000 hours must be satisfied (Critère 1 [116]).

Furthermore, the carbonyl absorbance was calculated relative to the CH_2 scissoring peak [117] occurring at 1465 cm^{-1} as a consequence of photo oxo-degradation, thermo oxo-degradation, thermo oxo-degradation with controlled humidity and effect of water. The results are expressed as the carbonyl index, which was calculated by Eq. 2.3.

$$\text{Carbonyl index} = \frac{A_{1715}}{A_{1465}} \tag{2.3}$$

where A_{1715} is absorbance of carbonyl peak at approx. 1715 cm^{-1} and A_{1465} is absorbance of CH_2 scissoring peak at approx. 1465 cm^{-1}.

2.4.2 Rheological properties

Whereas FTIR spectroscopy follows chemical changes, rheology is sensitive to observe already small increasing or decreasing of molecular weight of a chain. The reason is power law relationship between zero shear viscosity and molecular weight (let us say chain length) (see Eg. 1.13). Therefore, for degradation assessment comparison of η_0 is sufficient.

The changes in η' and η'' of degraded films were followed in oscillatory shear mode using a rotational controlled stress rheometer (StressTech, Rheologica Instruments AB) and controlled strain rheometer (ARES Rheometer, Rheometric Scientific) equipped with parallel plates geometry. The plate's diameter was 10 mm (StressTech) and 8 mm (ARES) and the gap between the plates was 1 mm. In all the cases, the values of the stress amplitude (StressTech) or strain amplitude (ARES) were checked to ensure that all measurements were conducted within the linear viscoelastic region. All the experiments were carried out at 180 °C and in ω range approx. 0.05 s^{-1} - 30 s^{-1}.

Changes of η^* components as a function of ω through the photo and thermo oxo-degradation of MF were measured. η_0 was obtained from an empirical Cole-Cole nonlinear regresion model (see Eq. 1.16) used to fit dynamic data (Prism® GraphPad Software).

2.4.3 Mechanical properties

Mechanical properties are effective determination of degradation of plastic; it is the most direct way between cause and consequence. The stressed importance of elongation at break during the life cycle of MF appears. However, any mechanical properties as a function of degradation are published seldom.

Mechanical properties were measured on specimens DCST, DC89, GDTP and DC55 in perpendicular direction to extrusion. Four specimens punched from each material even before degradation (photo oxo-degradation in SEPAP 12/24 at 60 °C and thermo oxo-degradation in the oven at 60 °C) were measured on MTS 200/M (Adamel Lhomargy). Standard flat dumbbell specimens with gauge length of approx. 30 mm, width of approx. 4 mm and thickness of approx. 0.01 mm were used. The measurements were carried out at ambient temperature (27 °C, 27 % RH). An initial crosshead speed of 1 mm/min to 1 % strain was used for accurate E-modulus determination. Then, the measurements continued at the crosshead speed of 100 mm/min. Only elongation at break and tensile stress at break are presented in this work.

2.4.4 Stereomicroscopy

Oxidized surface of films was examined by stereomicroscope (Stemi 2000-C, Zeiss). Specimens were observed under cool-light source (KL 1500, Zeiss). Owing to transparency of the films, side lighting was chosen. Oxidation of the films was obtained using 100-hour photo oxo-degradation in SEPAP 12/24 at 60 °C.

3 RESULTS AND DISCUSSION

The experimental results are presented in four sections. General evolution in chemical changes in the films upon various ways of degradation is followed by FTIR analysis in the first section. Rheological properties are discussed in the second section together with a tentative explanation of the relationship between recombination and chain scission. Mechanical properties of the films are shown in a subsequent section and finally, oxo-degradability is documented by stereomicroscopy in the last section.

3.1 FTIR analysis

The oxidation of polyethylene led to the accumulation of carbonyl groups. As shown in Figs. 3.1 – 3.8, the concentration of carbonyl groups can be used to monitoring the progress of degradation of mulching films.

3.1.1 Photo oxo-degradation

As defined in experimental part, material should be considered as a photo oxo-degradable if Eq. 2.2 is satisfied [Critère 2, 116]. Based upon this criterion and Fig. 3.1 (absorbance at 1716 cm^{-1} versus exposure time in SEPAP 12/24) only DC89, 10 PD, GDTP and DC55 mulching films are rated as photo oxo-degradable.

In Fig. 3.2 carbonyl index as a function of exposure time in SEPAP 12/24 is shown. It is evident that most of the mulching films showed similar IP (40 hrs). However, kinetics of oxidation after IP is significantly different in the samples under study. Within the exposure period in SEPAP 12/24, DGUV was found to be intact. DCN82 showed rather slight increase of the degradation by-products. DC55 manifested the most significant changes in chemical structure induced by combination of UV-light, heat and air. Consequently, after 120-hrs exposure the film was entirely disarticulated.

As the most photo oxo-degradable MF is considered DC55. Evidently, relative high photo oxo-degradability was recorded in the films DC89, 10PD and GDTP. In the case of DCST, DCRG and DCN82 the degradation proceeded quite slowly as demonstrated by a flat slope of carbonyl curves. DGUV film was unaffected in SEPAP 12/24.

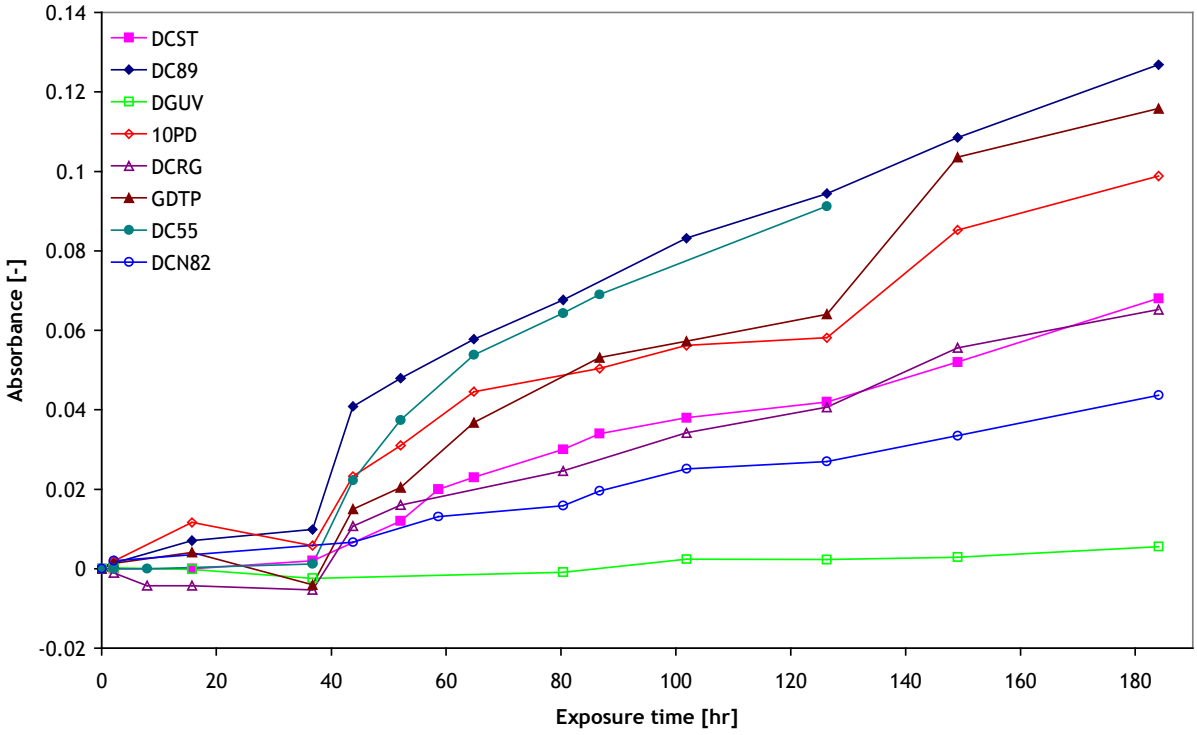

Fig. 3.1. Absorbance of carbonyl band as a function of exposure time in SEPAP 12/24.

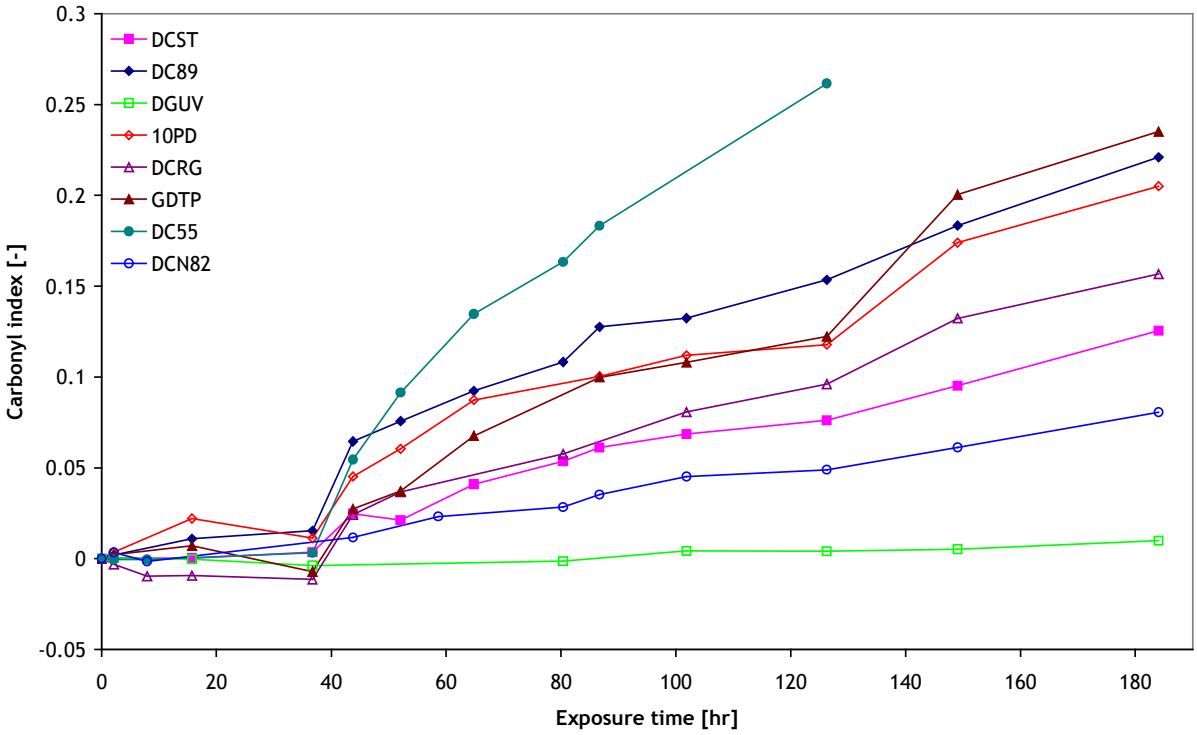

Fig. 3.2. Carbonyl index as a function of exposure time in SEPAP 12/24.

3.1.2 Natural ageing

No carbonyl by-products were detected in the most photo oxo-degradable films DC55 and DC89 after 7-day outside exposure (longer time was not available). During the test (23rd April – 30th April 2007) the weather was sunny and the average daily temperature was approx. 18 °C. It rained two times, each time for approx. 2 hours.

As a consequence of these negative results, it may be concluded that the IP during outdoor exposure is certainly longer than 7 days.

3.1.3 Thermo oxo-degradation

Based upon criterion in [Critère 1, 116] and Fig. 3.3 (absorbance at 1716 cm^{-1} versus exposure time in oven at 60 °C) all mulching films should be considered as a thermo oxo-degradable, except of 10PD.

As illustrated in Fig. 3.4, individual samples showed wide variation in both induction period and degradation kinetics upon exposure in the oven at 60 °C. While the films DC89 and DCRG displayed rapid carbonyl formation at the very beginning of heat exposure, the IP of the other samples was at least double. Long IP was found in DGUV sample. No formation of carbonyl products upon exposure was observed for 10PD.

With regard to the shape of curves, two main groups of films might be distinguished. The first group represented by s-shaped curve is typical for DC89 and DCRG. This trend indicates that the concentration of carbonyl products reached saturation level within the exposure applied and, the sample should be rated as entirely oxidised. The same shape of the curves should be expected for the other samples, if the exposure time will be adequately prolonged.

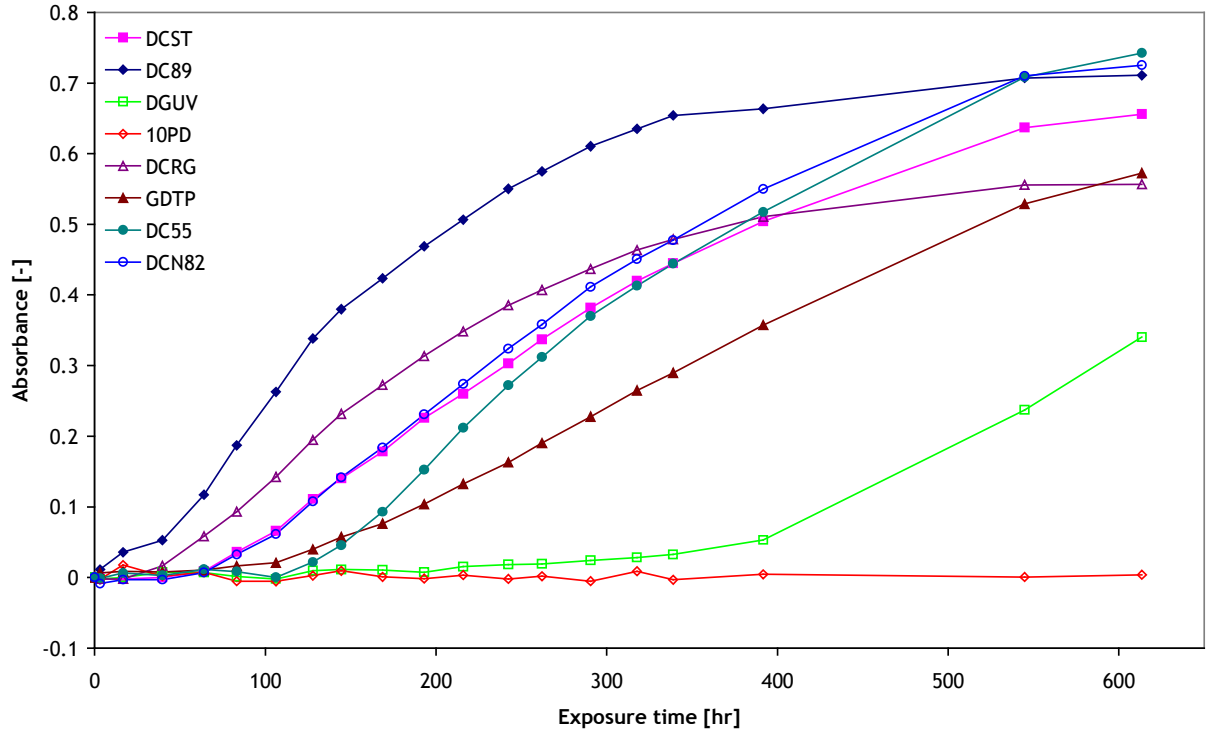

Fig. 3.3. Absorbance of carbonyl band as a function of exposure time in oven at 60 °C.

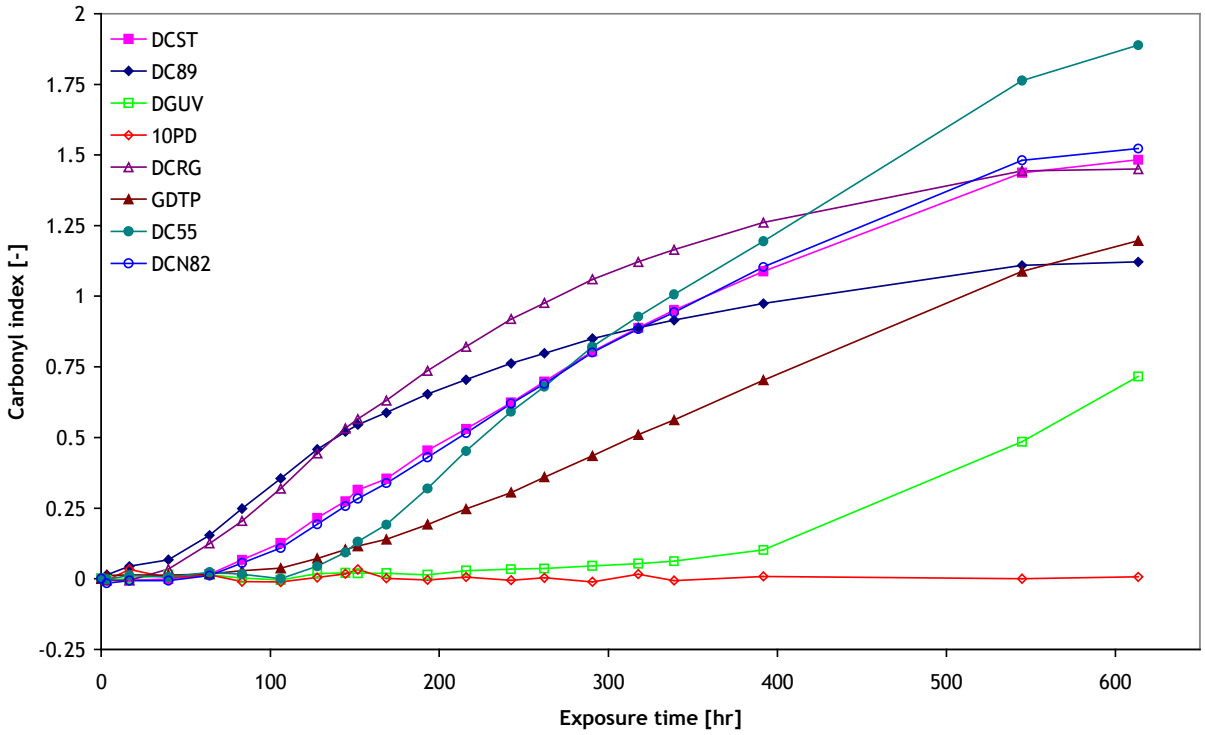

Fig. 3.4. Carbonyl index as a function of exposure time in oven at 60 °C.

3.1.4 Thermo oxo-degradation with controlled humidity

No evolution of carbonyl peak (see Fig. 3.5) was found in any mulching film during 61-day exposure in the oven with controlled humidity (80 °C, 70 % RH). These results indicate that the humidity inhibited thermal oxidation of mulching films. It should be pointed out that these results are inconsistent with many research works [7,53] reporting positive effect of humidity on thermo-oxidation. This discrepancy can be ascribed to the different course of oxidation in the materials under study resulting from their composition.

Obviously, it is hard to explain the inhibitory effect without more detailed study. However, it is generally known that polyethylene has relatively worse barrier properties. The humidity can permeate easily the amorphous regions of the film [74] and deactivate free radicals. Consequently, the formation of low molecular by-products such as carboxylic acids cannot proceed.

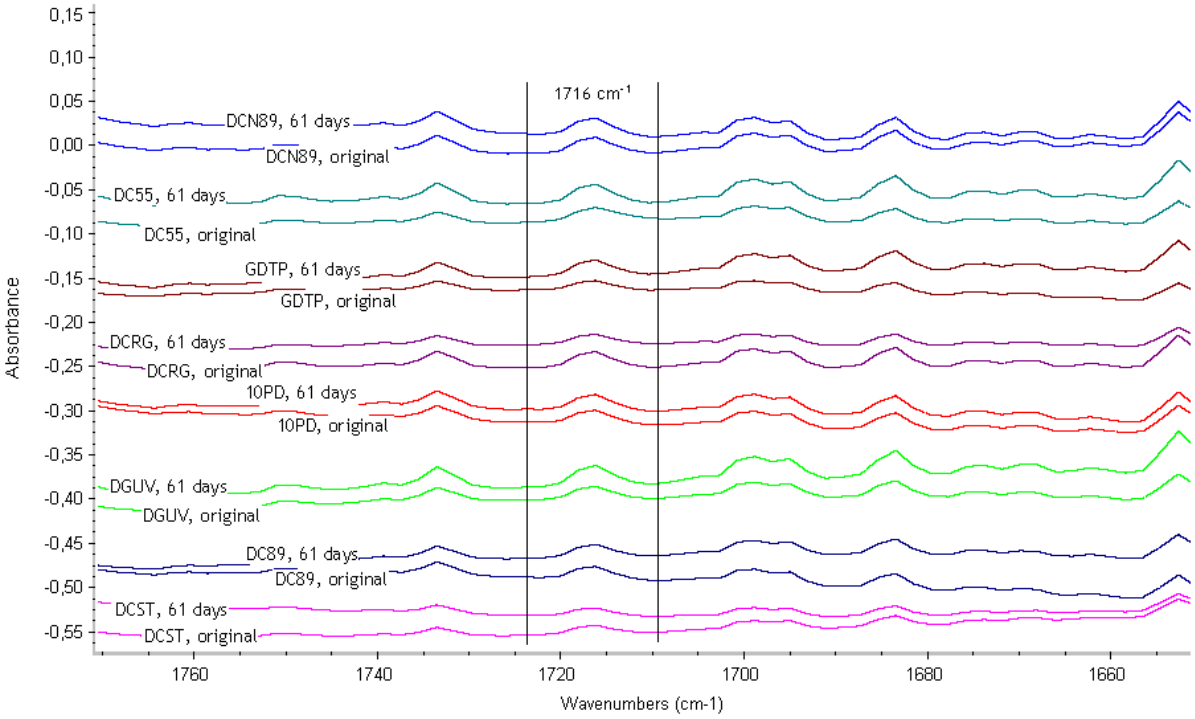

Fig. 3.5. *Carbonyl peak before and after 61-day exposure in oven with controlled humidity.*

3.1.5 Effect of water

Within real condition mulching film is often exposed to water. Simulation of the effect of water was performed by bathing the samples for 16 days in distilled water at either 20 or 60 °C. After that, the samples were exposed to the UV-light, heat and air in SEPAP 12/24. Fig. 3.6 shows the carbonyl index versus exposure time of the samples. It is obvious that the higher level of degradation was achieved in the samples bathed in water at 60 °C.

Figs. 3.7 and 3.8 compare the photo-oxidation of the as-processed samples and samples after the bathing. Generally, it can be seen that the water bathing brings a significant effect on the oxidation of the samples. It can be assumed that water led to the selective leaching of the antioxidants. However, no analyse of the leach water was done. The second effect, which should be taken into account, is the chemical modification of the ends of macromolecules accessible on the surfaces of materials upon water bathing. It can be supposed that the accrued groups like hydroxyls, carboxylic acids can act as chromophores during subsequent UV-exposure.

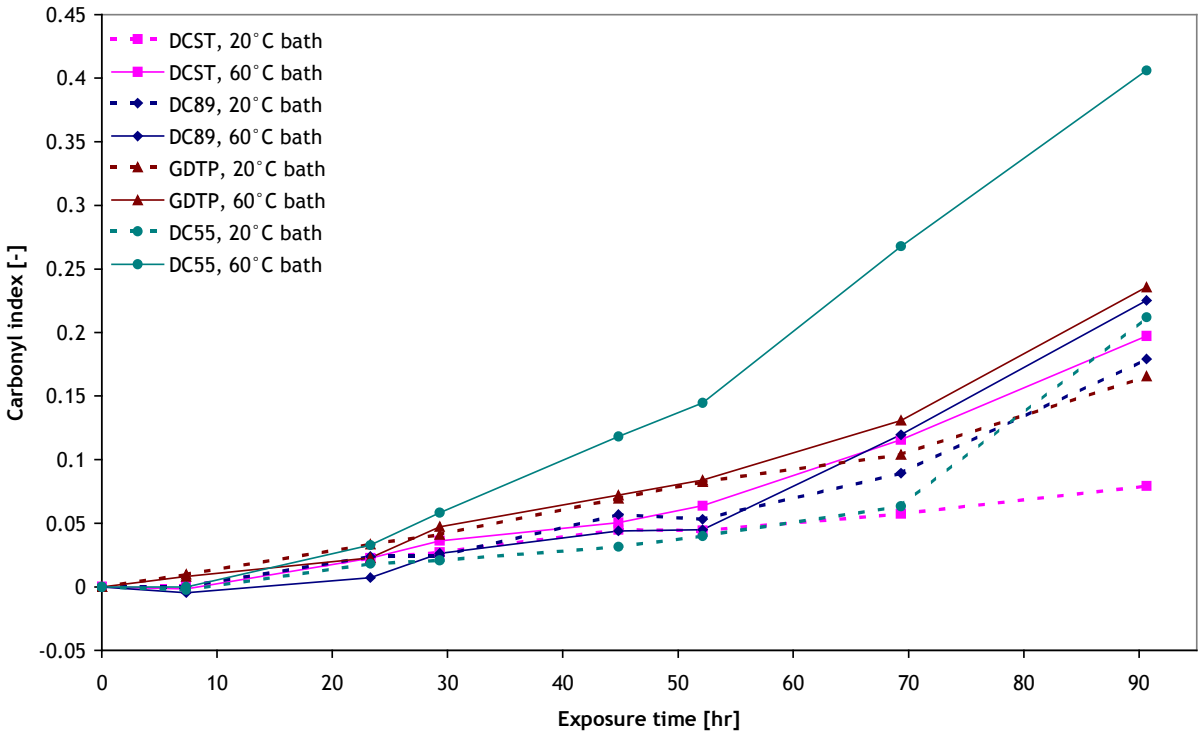

Fig. 3.6. *Carbonyl index as a function of exposure time in SEPAP 12/24 after 16-day bath in distilled water at 20 °C (broken line) and 60 °C (unbroken line).*

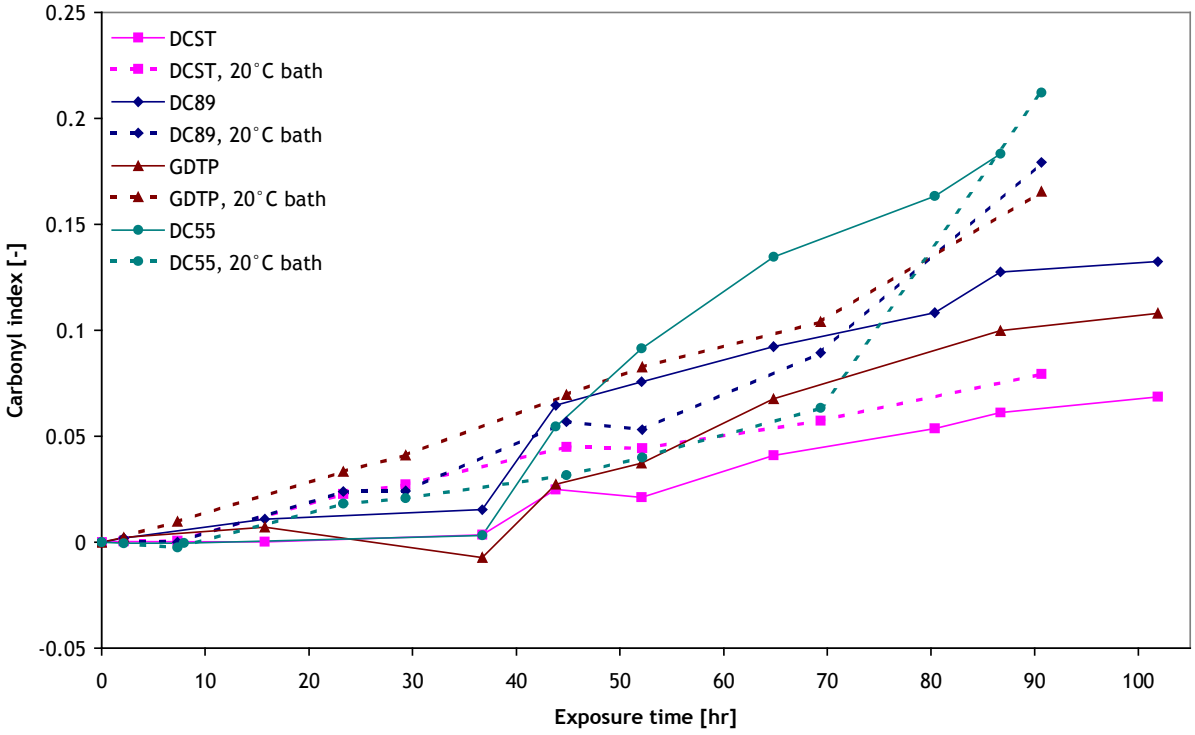

***Fig. 3.7**. Carbonyl index as a function of exposure time in SEPAP 12/24 after 16-day bath in distilled water at 20 °C (broken line). Unbroken line represents the as-proceesed specimen.*

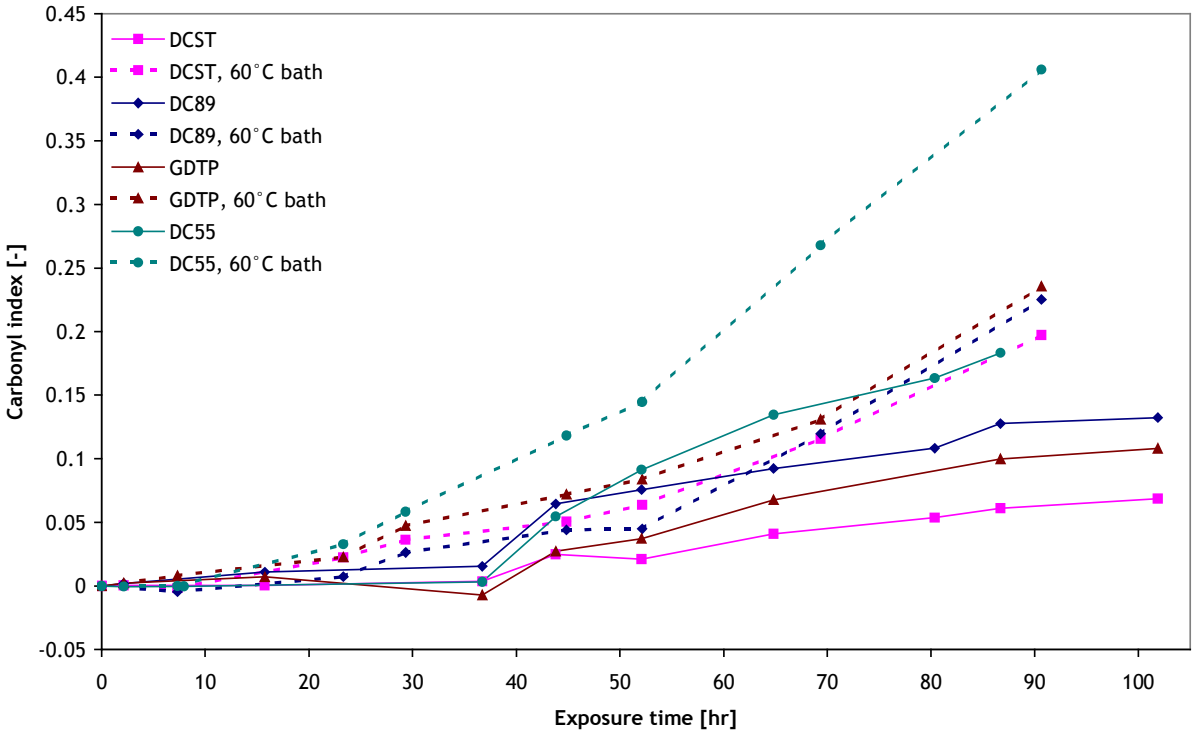

***Fig. 3.8**. Carbonyl index as a function of exposure time in SEPAP 12/24 after 16-day bath in distilled water at 60 °C (broken line). Unbroken line represents the as-proceesed specimen.*

3.2 Rheological properties

The degradation of MF is manifested in various ways. Chemical and physical changes occur and may be described by rheology. Analyses of zero shear viscosity changes give the degradation kinetics and make it possible to distinguish between chain recombination, involving crosslinking and chain scission. As discussed in theoretical background, the dependence of zero shear viscosity versus molecular weight obeys a power law (Eq. 1.13) but only in the case of supercritical molecular weight. Although the loss of molecular weight proceeded within oxidation, the changes should not result in the drop below the critical value (for polyethylene approx. 3,000 g mol^{-1}).

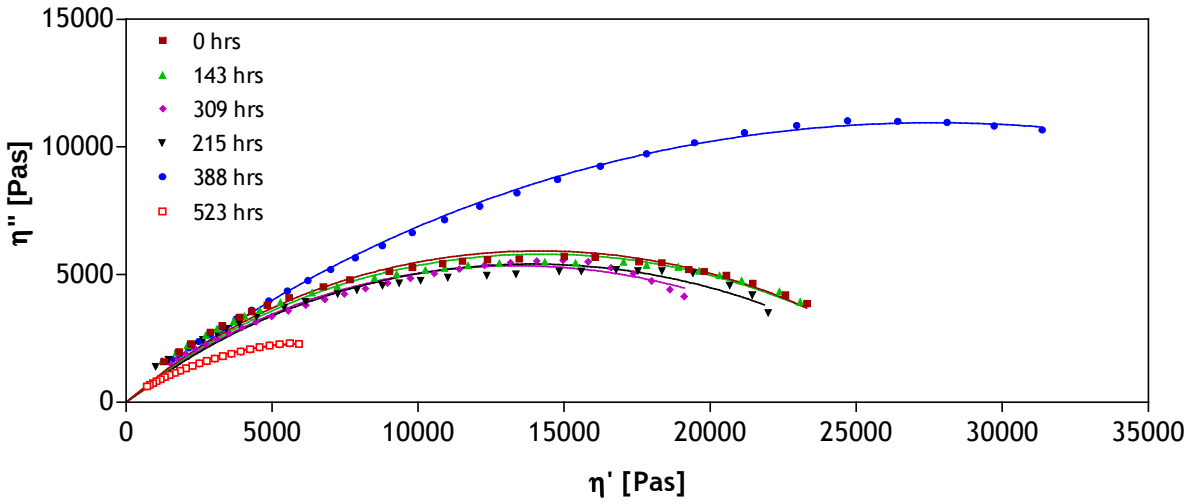

Fig. 3.9. *Changes of η* components through the thermo-oxidation in oven at 60 °C of GDTP film using the Cole-Cole representation for different exposure times.*

An evolution of complex viscosity components measured on GDTP film upon the thermo-oxidation is shown in Fig. 3.9. Cole-Cole representation for different exposure times was applied. Three main phases in dependence of molecular weight on degradation may be distinguished. At the beginning of the exposure, no relevant modification in chain length occurs reflecting subcritical concentration of free radicals in the system. Hence, the η_0 shows neglectable variation (see curves 0 – 215 hrs). When the amount of free radicals inside the system reach a sufficient level, the probability for recombination becomes to be high. Consequently, in the second phase, the η_0 increase provides evidence of a network formation (see curve 388 hrs). Finally, scission reactions are predominant as a result of wide peroxidation, and η_0 rapidly decreases (see curve 523 hrs). This course of the molecular changes can be generalized for all the samples under study.

Figs. 3.10 and 3.11 display the changes in η_0 versus exposure time in SEPAP 12/24. The photo oxo-degraded films show an almost immediate growth in η_0. It is obvious that the recombination involving possible crosslinking came at the very beginning of exposure, followed by chain scissions in the next stage. Fig. 3.12 and 3.13 show the behaviour of films upon thermo oxo-degradation in the oven. In comparison with the previous photo-degradation the maximum of η_0 is less pronounced. Moreover, the scission reactions are shifted toward the longer exposure time. This fact indicates a fast formation of free radicals in the films during photo oxo-degradation. Hence, the UV-light can be rated as dominant factor causing changes in the molecular structure of mulching films.

Regardless absolute value of η_0, similar kinetics of photo-degradation in DC89, 10PD, GDTP and DC55 may be supposed (see Figs. 3.10 and 3.11). After a rapid recombination, chain scission followed. Evidently, photo pro-oxidants are incorporated. As for DCST and DCRG, it can be seen that after gradual increase in η_0 within 80 hrs-exposure, decrease followed, therefore, an average kinetics of chemical changes might be supposed. Long recombination period in DGUV reflects non-photo oxo-biodegradability resulting from the possible presence of antiperoxidants. DCN82 show rather low photo oxo-degradability.

As mentioned above, the thermo-oxidation proceeded with slower kinetics, compared to that of photo-oxidation. Thus, the course of η_0 as a function of exposure time significantly differs in individual samples. Rapid decrease of η_0 and the lowest value was achieved in DC89 and DCRG and the highest thermo oxo-degradation was proved again. On the other hand, DGUV and 10PD showed the slowest degradation kinetics. Hence, peroxidolytic antioxidants that catalytically destroy POOH might be incorporated. The remaining films (DCST, GDTP, DC55, DCN82) displayed moderate kinetics in molecular changes induced by heat and oxygen. This is an important result and the prerequisite of distinct application of individual films.

All the results indicate that the linear viscoelastic properties may be used to characterise the changes in polymer structure. From the degradation kinetics viewpoint, the results from rheology are in good agreement with those of FTIR analysis.

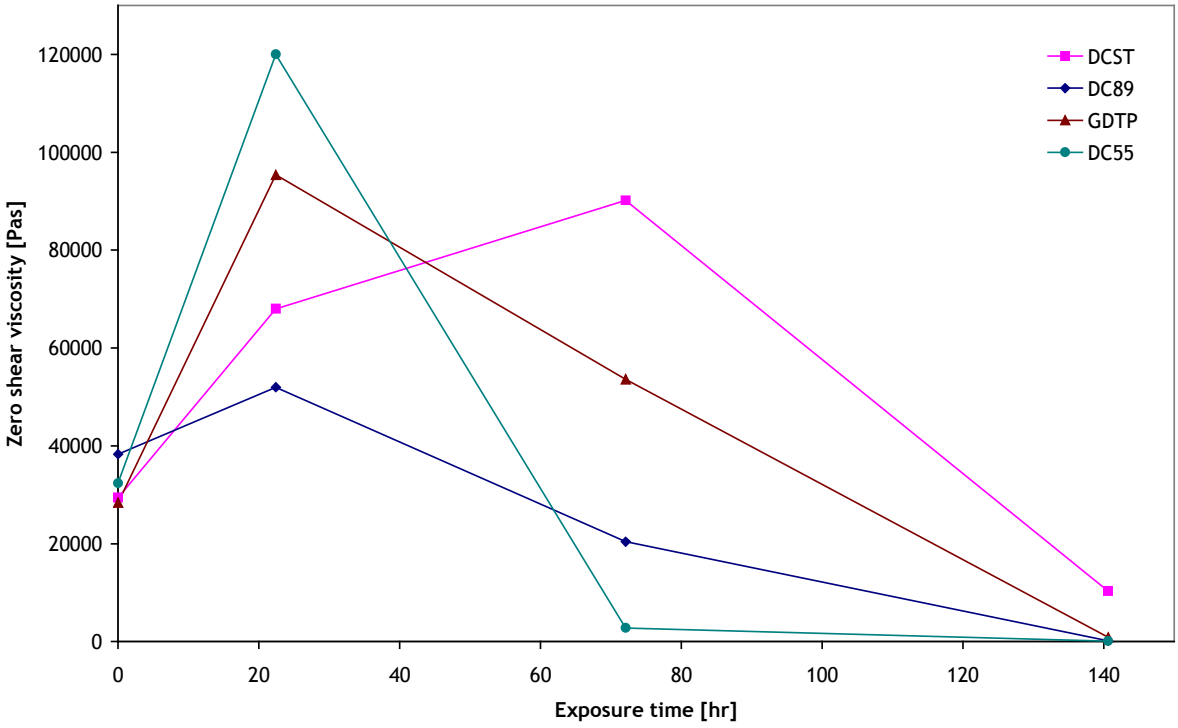

Fig. 3.10. Zero shear viscosity variation as a function of exposure time in SEPAP 12/24.

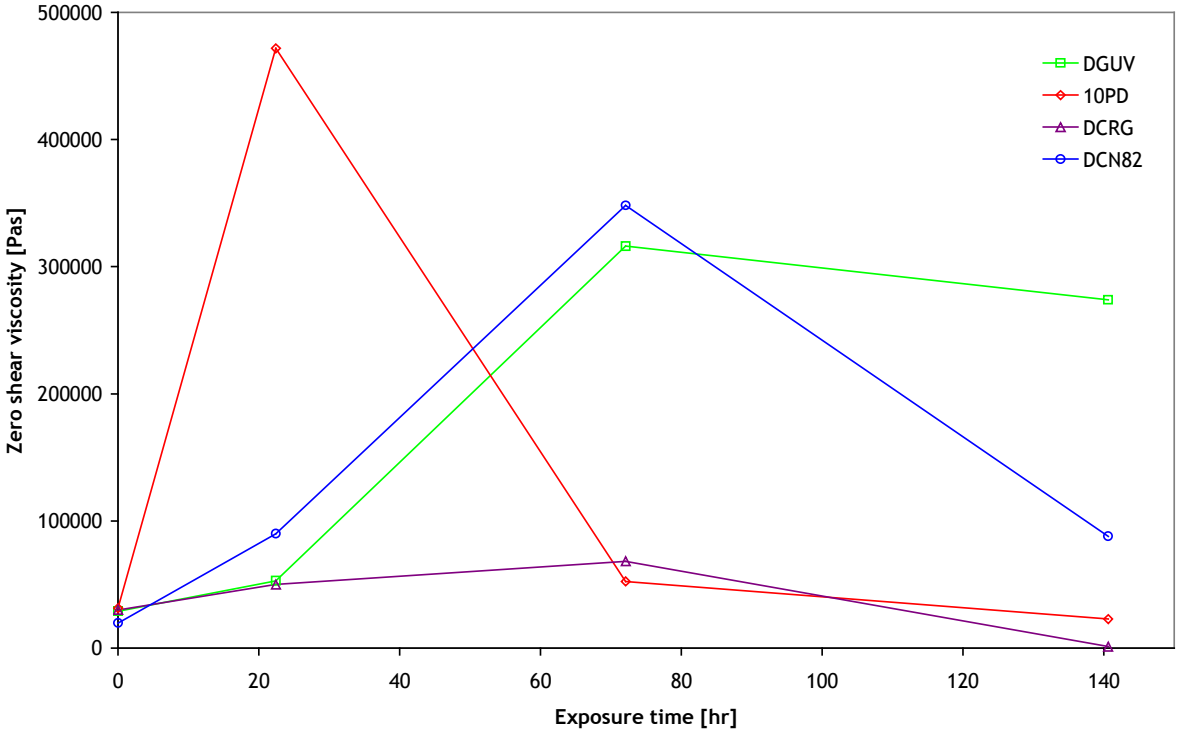

Fig. 3.11. Zero shear viscosity variation as a function of exposure time in SEPAP 12/24.

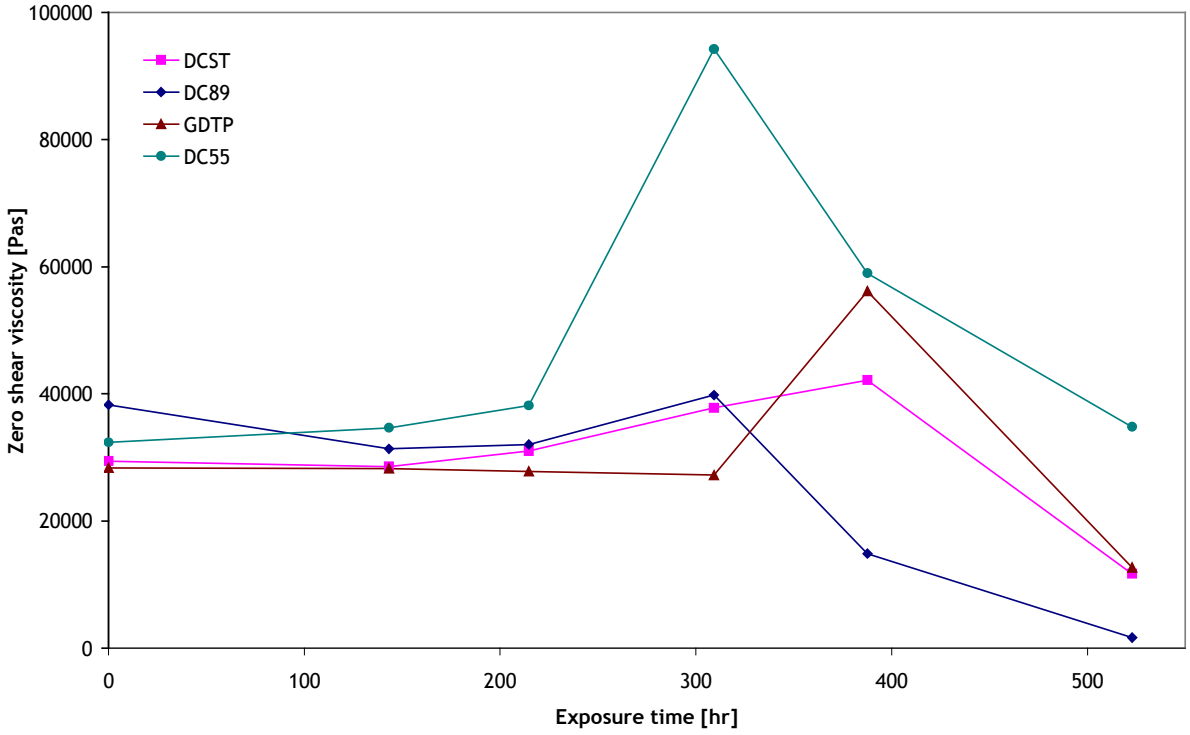

***Fig. 3.12**. Zero shear viscosity variation as a function of exposure time in oven at 60 °C.*

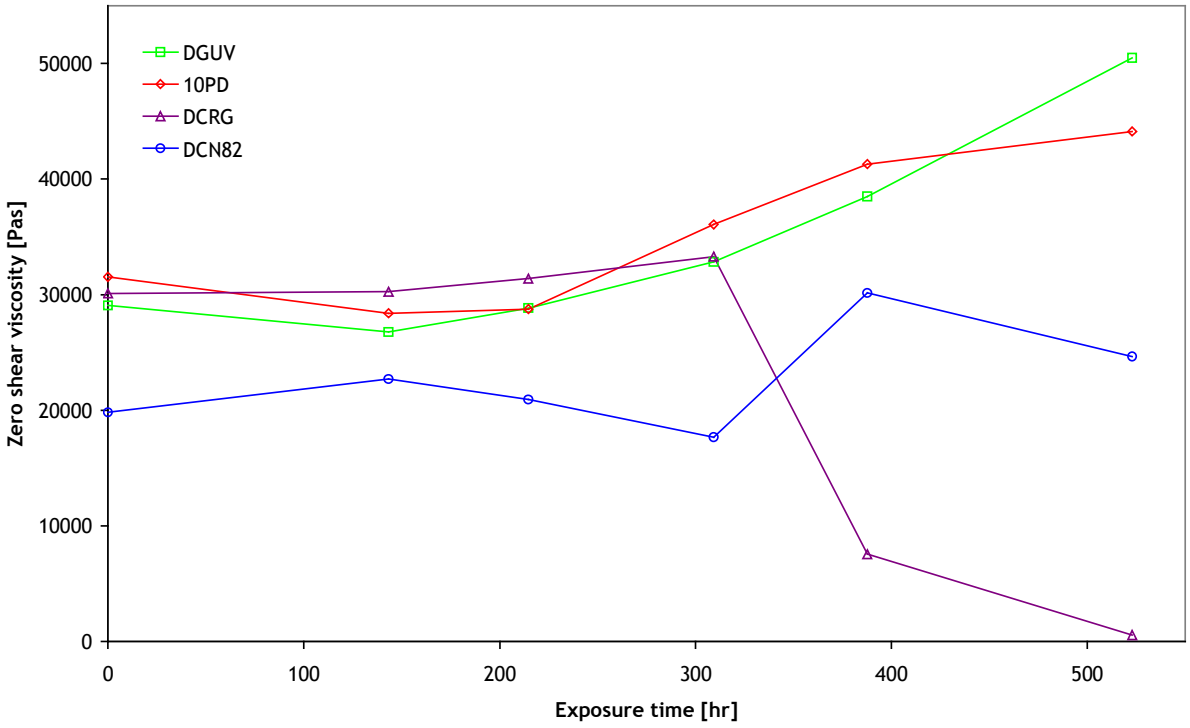

***Fig. 3.13**. Zero shear viscosity variation as a function of exposure time in oven at 60 °C.*

3.3 Mechanical properties

Oxo-degradation changes in mulching films are directly manifested in mechanical properties. From the stress-strain diagrams elongation at break and tensile stress at break were calculated. The elongation at break as a function of exposure time in SEPAP 12/24 is presented in Fig. 3.14. Correspondingly, Fig. 3.15 shows dependence of elongation at break on exposure time in the oven at 60 °C.

Rapid drop of elongation at break appeared in the DC89 and DC55 specimens. This behaviour was observed for both photo- and thermo-oxidation. A remarkably slower deterioration of mechanical properties upon photo-oxidation was observed for DCST and GDTP. On the contrary, a slight increase in elongation at break during 3-day exposure in oven was recorded for these samples. Presumably, the increase of drawability might be coupled with the modification of chain length or crosslinking. These results are practically important because mechanical properties during the whole growing season should be steady. Nevertheless, further photo and thermo oxo-degradation led to drop of mechanical properties. This can be ascribed to the formation of cracks and low molecular weight (by-) products resulting from the physical and chemical changes.

Stress at break was only measured for the samples prior exposure, because the original values should satisfy the conditions defined by European Standard [118]. For PE mulching films, the minimum value of stress at break is defined to be at least 16 MPa. As can be seen from the Table 3.1. all the measured mulching films showed higher values.

Table 3.1. *Original tensile stress at break.*

MF	Tensile stress at break [MPa]
DCST	48 ± 3
DC89	34 ± 1
GDTP	51 ± 6
DC55	49 ± 3

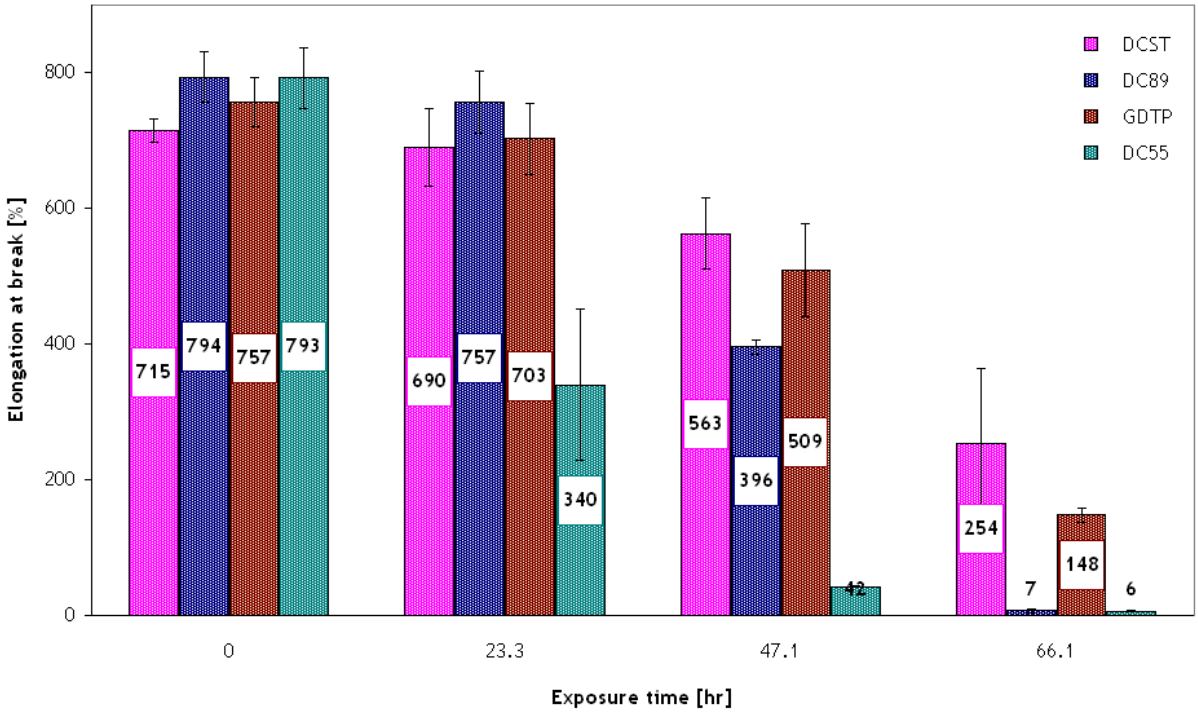

***Fig. 3.14**. Elongation at break variation as a function of exposure time in SEPAP 12/24.*

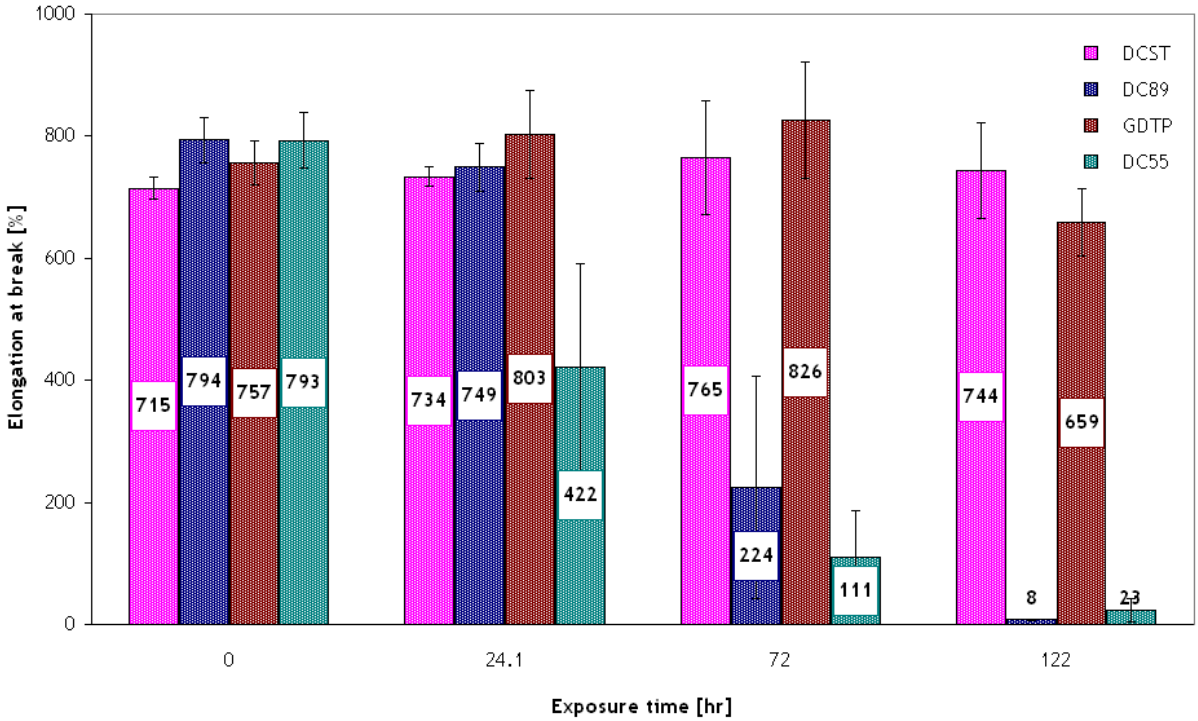

***Fig. 3.15**. Elongation at break variation as a function of exposure time in oven at 60 °C.*

3.4 Steromicroscopy

Surface of photo-oxidized mulching films was examined by stereomicroscopy under 40× magnification. The micrographs of photo-oxidized films are presented in Fig. 3.16. As can be seen from comparison of the original and exposed DCN82, the degradation is expressed by white marks resulting from the formation of cracks and low molecular products. Therefore, it can be assumed that the percent occurrence of this white marks correlates with oxo-degradation of mulching films. Evidently, the highest photo-oxidation is manifested in DC55 whereas DGUV seems to be intact. This result corresponds to that of FTIR analysis and rheology. Thus, stereomicroscopy can be used for the estimation of the oxo-degradation extent.

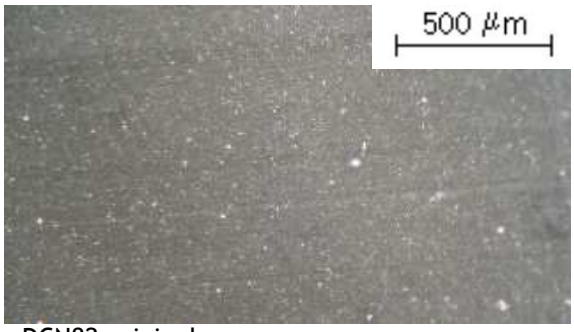

DCN82 original

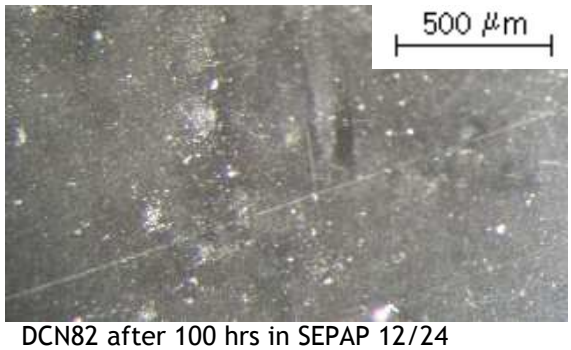

DCN82 after 100 hrs in SEPAP 12/24

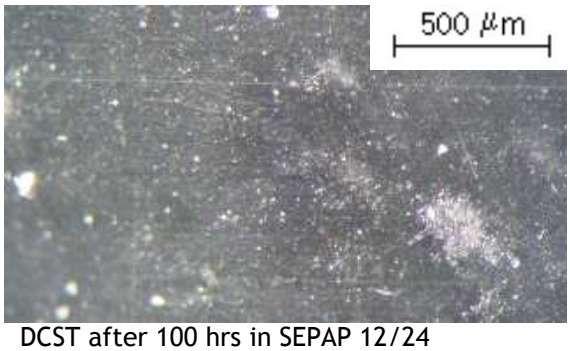

DCST after 100 hrs in SEPAP 12/24

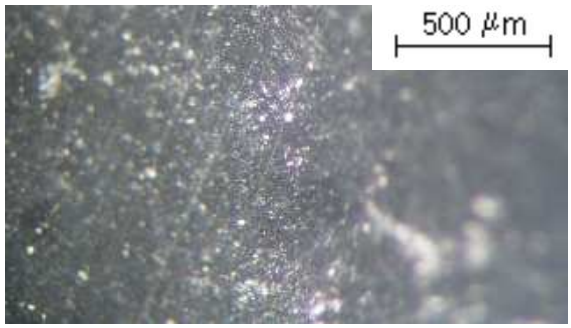

DC89 after 100 hrs in SEPAP 12/24

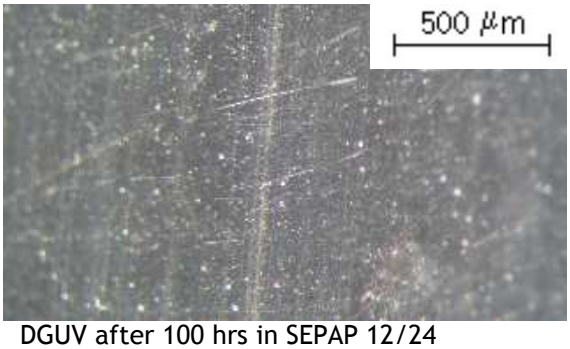

DGUV after 100 hrs in SEPAP 12/24

10PD after 100 hrs in SEPAP 12/24

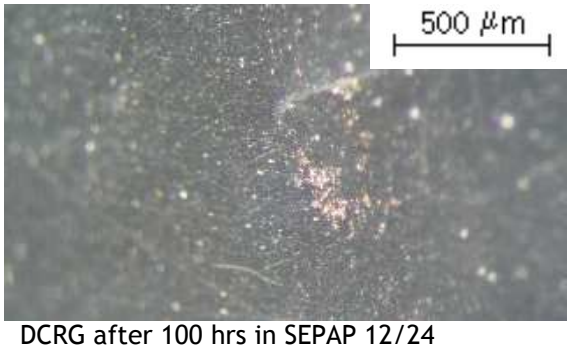

DCRG after 100 hrs in SEPAP 12/24

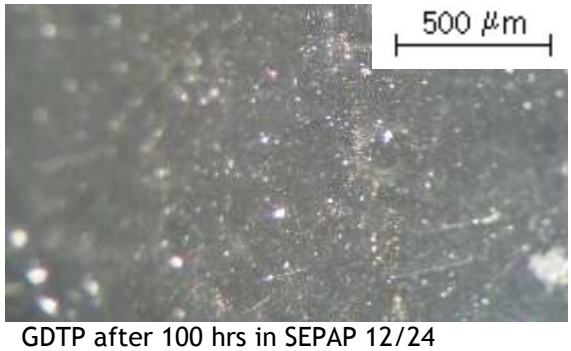

GDTP after 100 hrs in SEPAP 12/24

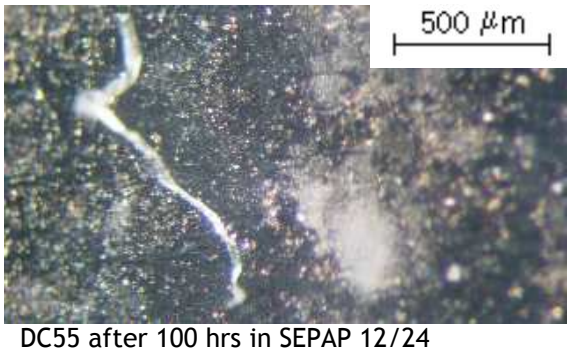

DC55 after 100 hrs in SEPAP 12/24

Fig. 3.16. *Stereomicroscopy demonstration of the oxo-degraded film surface.*

CONCLUSION

Eight types of commercially available mulching films were exposed to UV-light, heat, humidity and water. Resulting changes in chemical, physical and mechanical properties were thoroughly characterized by the combination of several analytical methods. Although the certain formulation of the samples has not to be published, the main conclusion can be drawn as follows:

- Mulching films showed significant differences in degradation kinetics reflecting variation in type, amount and combination of additives.
- FTIR analysis confirmed that both photo and thermo oxo-degradation resulted in formation of low-molecular by-products.
- Changes in molecular weight upon abiotic oxidation were followed by rheology. Increase of viscosity evidenced the recombination processes within early stage of degradation, while the chain scission was manifested by the fall in viscosity with prolonged exposure.
- Drop of mechanical properties was ascribed to the reduction in molecular weight and formation of cracks upon exposure.
- Air humidity was found to be an inhibitory factor for thermo oxo-degradation. Within already published papers, such behaviour has not been described yet. On the other hand, exposure to water resulted in faster formation of oxidative by-products in films during subsequent photo oxo-degradation. From application point of view, these results are particularly important; essential humidity maintained under the mulching films during the growing season does not increase oxo-degradability, consequently, no changes in mechanical properties proceeds; by contrast, the water either as rain or in the soil supports the degradation of films residues after harvest.

The relative oxo-degradability of individual mulching films is summarized in Appendix I.

Finally, it has to be pointed out that the main goal is not to find the material with the highest degradability. These materials represent a new branch of polymeric materials with time-controlled life cycle. Therefore, the idea is to meet the durability with the service time of the mulching films.

REFERENCES

[1] Raab M. Materiály a člověk: Encyklopedický dům, Praha; 1999.

[2] http://www.plasticseurope.org/Content/Default.asp?PageID=92.

[3] Curlee TR, Das S. Plastic Wastes - Management, Control, Recycling and Disposal: William Andrew Publishing, Noyes; 1991.

[4] Environmental Engineering: John Wiley & Sons, Inc., New Jersey; 2003.

[5] Jagger A. Plastic Surgery: ICIS Chem Bus Amer 2007;271:54-55.

[6] Boustead I. Plastics and the environment: Radiat Phys Chem 1998;51:23-30.

[7] Jakubowicz I, Yarahmadi N, Petersen H. Evaluation of the rate of abiotic degradation of biodegradable polyethylene in various environments: Polym Degrad Stab. Article in press.

[8] Gerngross TU, Slater SC. How green are green plastics?: Scientific American; 2000.

[9] Angold R. The fate of carbon from the breakdown of degradable polyolefin plastics: a biologist's view: Pyxis CSB Ltd., Oxfordshire; 2006.

[10] Wittwer SH. World-wide use of plastics in horticultural production: HortTechnology 1993;3:6-27.

[11] Holmes M. Increasing use of plastics in agriculture. Available onwww.p2pays.org/ref/33/32205.pdf.

[12] Jouët JP. Plastics in the world: Plasticulture 2001;120:108-126.

[13] CIPA. Plasticulture comes of age: Plast Addit & Comp 2005;32:16-19.

[14] Dalrymple DG. A global review of greenhouse food production: USDA Rpt. 89; 1973.

[15] Jensen MH. Plasticulture in the Global Community - View of the Past and Future. Available onhttp://www.plasticulture.org/history_global_community.htm.

[16] http://www.uaf.edu/salrm/afes/pubs/rpr/RPR%252025.pdf.

[17] Sheldrake R, Langhans R. Heating study with plastic greenhouses. Proc Nat Hort Plastics Cong 1961;2:16-17.

[18] Roberts WJ, Mears DR. Double covering a film greenhouse using air to separate film layers: Trans Amer Soc Agric Eng 1969;12:32-38.

[19] Mansour NS. The use of field covers in vegetable production: Proc Intl Workshops on Imp Veg Prod Through the Use of Fert Mulching and Irrigation: Chaing Mai Univ, Thailand; 1991.

[20] Jensen MH, Valenzuela M, Fangmeier DD. Using non-woven floating covers on summer squash for exclusion of whitefly - transmitted gemini viruses: Proc Nat Agric Plastics Cong 1998;27:159-164.

[21] Morrison CT, Green WT, Hadley P. Energy exchange by plastic row covers: Proc Nat Agric Plastics Cong 1989;21:269-275.

[22] Thompson HC, Kelly WC. Vegetable Crops: McGraw-Hill Book Co. Inc., New York; 1957.

[23] Decoteau DR, Kasperbaur MJ, Hunt PG. Mulch surface color affects yield of fresh-market tomatoes: J Amer Soc Hort Sci 1989;114:216-219.

[24] Orzolek MD, Murphy JH. The effect of colored polyethylene mulch on the yield of squash and pepper: Proc Nat Agric Plastics Cong 1993;24:157-161.

[25] Loy B, Lindstrom J, Gordon S, Rudd D, Wells O. Theory and development of wavelength selective mulches: Proc Nat Agric Plastics Cong 1989;21:193-197.

[26] Gilead D, Scott G. "Time controlled stabilisation of polymers" in Scott G, eds. Developments in Polymer Stabilisation, App Sci Pub Barking; 1989.

[27] Fabri A "The role of degradable polymers in agricultural systems" in Scott G, Gilead D, eds. Degradable Polymers: Principles and Applications, eds. Scott G, Gilead D, Chapman and Hall: Kluwer Acad Pub; 1995.

[28] Scott G, Wiles DM "Degradable carbon polymers in waste and litter control" in Scott G, Gilead D, eds. Degradable polymers: Principles and applications, Chapter 13: Chapman & Hall; 2002.

[29] Agricultural Statistics Yearbook (2001).

[30] Yang SR, Wu CH. Degradable plastic films for agricultural application in Taiwan: Degradability, Renewability and Recycling, 5th International Scientific Workshop on biodegradable Plastics and Polymers, Macromolecular Symposia, eds. Albertsson AC, Chiellini E, Feijen J, Scott G, Vert M: Wiley-VCH;101-112.

[31] Environmental Technologies Action Plan, July 2006. Available on http://ec.europa.eu/environment/etap.

[32] Scott G. The Role Biodegradable Plastics in Agriculture, A brief review: Aston University, Birmingham.

[33] Gilead D. "Photodegradable plastics in agriculture" in Scott G, Gilead D, eds. Degradable polymers: Principles and applications: Chapman & Hall; 1995.

[34] Casaliccio GH, Bertoluzzo A, Fabbri A. Photodegradable film research – Initial research into the possible toxic effect of photodegradability inductors on sweet corn and melons: Plasticulture 1990;86:21-28.

[35] Casaliccio GH, Bertoluzzo A, Fabbri A. Photodegradable film research – Further research into the possible toxic effect of photodegradability inductors on potatoes and canning tomatoes: Plasticulture 1990;87:47-53.

[36] Taber HG, Ennis R. Plant uptake of heavy metals from decomposition of Plastigone™ photodegradable plastic mulch; Proc. N.A.P.A Conference Orlando1989;47.

[37] Yang SR. Personal communication; 2000.

[38] Scott G. Polym Age 1975;6:54.

[39] Albertsson AC. Pure Appl Chem 1993;A30(9 & 10):757.

[40] Jakubowicz I. Evaluation of degradability of biodegradable polyethylene (PE): Polym Degrad Stab 2003;80:39–43.

[41] Scott G. Abiotic control of polymer biodegradation: Trends in Polymer science 1997;5:361-368.

[42] Arnaud R, Dabin P, Lemaire J, Al-Malaika S, Chohan S, Coker M, Scott G, Fauve A, Maaroufi A. Photooxidation and biodegradation of commercial photodegradable polyethylenes: Polym Degrad Stab 1994;46:211.

[43] Scott G. Biodegradable polymers, Polymers and the environment: Royal Society of Chemistry Paperbacks; 1999.

[44] Scott G. “Degradation and stabilisation of carbon-chain polymers” in Scott G, eds. Degradable polymers: Principles and application: Kluwer Acad Pub; 2002.
[45] Bonhomme S, Cuer A, Delort AM, Lemaire J, Sancelme M, Scott G. Environmental degradation of polyethylene: Polym Degrad Stab 2003;81:441-452.
[46] Weiland M, Daro A, David C. Polym Degrad Stab 1995;48:275-289.
[47] Albertsson AC, Barenstedt C, Karlsson S, Lindberg T. Polymer 1995;36:3075-3083.
[48] Karlsson S, Albertsson AC. Polym Eng Sci 1998;38:1251-1253.
[49] Chiellini E, Corti A, Swift G. Polym Degrad Stab 2003;81:341-351.
[50] Wiles DM. Biodegradable polymers for industrial applications: Woodhead Publishing, Cambridge; 2005.
[51] Scott G. Green Polymers: Polym Degrad Stab 2000;68:1-7.
[52] Scott G, Wiles DM. Biomacromolecules 2001;2:615-622.
[53] Chiellini E, Corti A, D’Antone S, Baciu R. Oxo-biodegradable carbon backbone polymers – Oxidative degradation of polyethylene under accelerated test conditions: Polym Degrad Stab 2006;91:2739-2747.
[54] Iring M, Foldes E, Barabas K, Kelen T, Tudos F. Thermal oxidation of linear low density polyethylene: Polym Degrad Stab 1986;14:319-332.
[55] Winslow FH. Photooxidation of high polymers: Pure Appl Chem 1977;49:495-502.
[56] Sipinen AJ, Rutheford DR. Proc Am Chem Soc 1992;67:185–187.
[57] Khabbaz F, Albertsson AC, Karlsson S. Polym Degrad Stab 1998;61:329–342.
[58] Khabbaz F, Albertsson AC, Karlsson S. Polym Degrad Stab 1999;63:127–338.
[59] Koutny M. Biodegradace polyetylenu s prooxidanty: Plasty a kaučuk 2007;44:68-71.
[60] Khabbaz F, Albertsson AC. Biomacromolecules 2002;1(4):665– 673.
[61] Scott G. “Photo-biodegradable plastics” in Scott G, Gilead D, eds. Degradable polymers: Principles and Applications: Chapman & Hall; 1995.
[62] Grassie N, Scott G. Polymer Degradation and Stabilisation: Cambridge University Press; 1985.
[63] Scott G. “Photodegradation and photostabilisation of polymers” in Scott G, ed. Atmospheric Oxidation and Antioxidants: Elsevier; 1993.
[64] Scott G. Antioxidants in science, technology, medicine and nutrition: Albion Publishing, Chichester; 1997.
[65] Wiles DM, Scott G. Polyolefins with controlled environmental degradability: Polym Degrad Stab 2006;91:1581-1592.
[66] Dilara P A; Briassoulis D. Degradation and stabilization of low density polyethylene (LDPE) films used as greenhouse covering materials: Journ Agric Engin Res 2000;76:309–321.
[67] Rabek F. Polymer Photodegradation. Mechanisms and Experimental Methods: Chapman & Hall, London; 1995.
[68] Gugumus F. “Developments in the UV-stabilization of polymers” in Scott G, eds. Developments in Polymer Stabilisation: Elsevier Applied Science, Amsterdam; 1979.
[69] Khan JH, Hamid SH. Durability of HALS-stabilized polyethylene film in a greenhouse environment. Polym Degrad Stab 1995;48:137–142.
[70] Jones PH, Prasad D, Heskins M, Morgan MH, Guillet JE. Environ Sci Technol 1974;8:919.

[71] Omichi H. Degradation and stabilization of polyolefins: Applied Science Publishers, London; 1983.
[72] Rabek F. Photodegradation of Polymers. Physical Characteristics and Applications: Springer, Berlin; 1996.
[73] Briassoulis D, Aristopoulou A. A modified artificial ageing procedure for low density polyethylene (LDPE) agricultural films: Eur Ag Eng Conference Hungary 2002.
[74] Hamid SH, Amin MB, Maadhah AG. Handbook of Polymer Degradation: Marcel Dekker, New York; 1992.
[75] Al-Malaika S, Marogi AM, Scott G. J Appl Polym Sci 1986;31:685.
[76] Gilead D, Scott G, eds. Developments in Polymer Stabilization: Applied Science 1982;5:71.
[77] Briassoulis D, Aristopoulou A, Bonora M, Verlodt I. Degradation Characterisation of Agricultural Low-density Polyethylene Films: Biosystems Engineering 2004;88:131–143.
[78] Ram A. Fundamentals of Polymer Engineering: Springer – Verlag; 1997.
[79] Brydson J. Plastics Materials: Elsevier; 1997.
[80] Neway N. Doctoral Thesis: The Influence of Morphology on the Transport and Mechanical Properties of Polyethylene: Royal Institute of Technology; 2003.
[81] Fawcett EW. Trans Faraday Soc 1936;32:119.
[82] Ziegler KE. Angew Chem 1955;67:426-541.
[83] Brydson JA. Plastics materials: Butterworth-Heinemann, Oxford; 1999.
[84] Severin N. Doctoral Thesis: Molecular Dynamics Simulations of Polymers and Micelles at Interfaces: Humbolt-Universität zu Berlin. Mathematisch-Naturwissenscheftlichen Fakultät I; 1998.
[85] Lien-Vien D, Colthup NB, Fateley WG, Grasselli JG. The Handbook of Infrared and Raman Characteristic Frequencies of Organic Molecules: Academic Press, Inc., San Diego; 1991.
[86] King PL, Ramsey MS, McMillan PF, Swayze G. Laboratory fourier transform infrared spectroscopy methods for geologic samples. Available on http://ivis.eps.pitt.edu/ramsey/papers/GAC2.pdf.
[87] Klouda P. Moderní analytické metody: Pavel Klouda, Ostrava; 1996.
[88] Phan H. Fundamental infrared spectroscopy. Available on http://www.midac.com/apnotes/Tn-100.PDF.
[89] http://hyperphysics.phy-astr.gsu.edu/hbase/phyopt/michel.html.
[90] Åmand LE, Tullin CJ. The Theory Behind FTIR analysis: University of Technology Göteborg, Sweden.
[91] Bingham EC. The history of the Society of Rheology from 1924 – 1944; 1944.
[92] Scott Blair GW. Survey of general and applied rheology: Sir Isaac Pitman & Sons, London; 1949.
[93] Reiner M. The Deborah Number: Physics Today 1964;17:62.
[94] Doraiswamy D. The origins of rheology: A short historical excursion: Rheological Bulletin 2002;71:1-9.
[95] Colloid Science - Principles, Methods and Applications: Blackwell Publishing; 2005.
[96] Macosko CW. Principles, Measurements and Applications: Wiley-VCH, New York; 1994.

[97] Bird RB, Stewart WE, Lightfoot EN. Transport Phenomena: Wiley, New York; 1960.
[98] Goodwin JW, Hughes R. Rheology for Chemists, An Introduction: The Royal Society of Chemistry, Cambridge; 2000.
[99] Szabo JRP, Hinch E. Start-up of flow of a fene-fluid through a 4:1:4 constriction in a tube: Journal of Non-Newtonian Fluid Mechanics 1997;72:73.
[100] Michele RDJ, Pätzold R. Alignment and aggregation effects in suspensions of spheres in non-newtonian media: Rheol Acta 1977;16:317.
[101] Ferry JD. Viscoelastic properties of polymers: J Wiley, New York; 1970.
[102] Vinogradov GV, Malkin AY. Rheology of polymers: Springer, Berlin; 1980.
[103] Giesekus HW. Proc 4th Intern Congress Rheology: Interscience 1965;3:15-28.
[104] Verney V, Michel A. Representation of the rheological properties of polymer melts in terms of complex fluidity: Rheol Acta 1989;28:55-60.
[105] Winter HH. Gel point in encyclopedia of polymer science and engineering: John Wiley & Sons, New York; 1989.
[106] Commereuc S, Verney V, Kumar A. Ageing of elastomers: a molecular approach based on rheological characterization: Polym Degrad Stab 2004;85:751-757.
[107] Verney V, Michel A. 3rd annual meeting: Polym Proc Soc, Stuttgart; 1987.
[108] Cole KS, Cole RH. J Chem Phys 1974;9:341.
[109] Stűwe HP, Tóth LS. Plastic instability and Lűders bands in the tensile test: the role of crystal orientation: Mat Sc and Eng 2003;358:17-23.
[110] http://www.instron.us/wa/applications/test_types/tension/default.aspx.
[109] Harrison HR, Nettleton T. Principles of Engineering Mechanics: Elsevier; 1994.
[110] Rybnikář F. Analýza a zkoušení plastických hmot: SNTL, Praha; 1965.
[111] http://www.ni.com/pdf/academic/us/me105_lab3_2003.pdf.
[112] ČSN EN ISO 527-1.
[113] ČSN EN ISO 527-2.
[114] ČSN EN ISO 527-3.
[115] SEPAP 12/24, Brochure.
[116] CNEP. Règlement d'usage, ANNEXE II. Définition du cahier des charges du produit NEOSAC; 2005.
[117] Krishna SP, Satyanarayana D, Mohan RDV: J Appl Polym Sci 1998;70:2251-2257.
[118] EN-13655 Plastics. Mulching thermoplastic films for use in agriculture and horticulture. Brussels: Comite´ Europe´en de Normalisation (C.E.N.); 2002.

LIST OF SYMBOLS

A	absorbance or area
A_C	corrected absorbance
A_0	absorbance before exposure
A_{100}	absorbance after 100-hour exposure without IP
A_{1465}	absorbance at 1465 cm^{-1}
A_{1715}	absorbance at 1715 cm^{-1}
B	intensity of the source
c	velocity of light
c_M	molar concentration
Cat	catalysis
C	carbon
De	Deborah number
E	modulus of elasticity
F	force
FTIR	Fourier Transform Infrared
G	shear modulus
G′	storage modulus
G″	loss modulus
G*	complex modulus
h	parameter of relaxation time distribution
hν	photolysis
H	hydrogen
HDPE	high-density polyethylene
i	imaginary unit
iPP	isotactic polypropylene
I	intensity of the beam
IP	induction period
IR	Infrared
IRT	Infrared transmitting
l	cell thickness
L	length
LDPE	low-density polyethylene
LLDPE	linear low-density polyethylene
L_0	initial length
MF	mulching films
M_w	molecular weight

O_2	oxygen (gas)
PE	polyethylene
PET	polyethylene terephthalate
PH	carbon backbone polymer
PO	polyolefins
POOH	polymer hydroperoxides
PS	polystyrene
PVC	polyvinyl chloride
t	observation time
t_{s0}	thickness of standard specimen before degradation
t_0	thickness of existent specimen before degradation
T	transmittance
UTS	ultimate tensile strength
UV	ultraviolet
x	mirror displacement
α	angle or exponent
δ	loss angle
Δ	thermolysis
ΔL	elongation
ε	strain
ε_λ	absorptivity
Φ	intensity of the transmitted radiation
Φ_O	intensity of the entering radiation
γ	(shear) strain
$\dot{\gamma}$	strain rate
η	(shear) viscosity
η_0	zero shear viscosity
η'	storage viscosity
η''	loss viscosity
η^*	complex viscosity
λ	wavelength
λ_0	relaxation time
ν	frequency
$\overline{\nu}$	wavenumber
σ	(shear) stress
τ	relaxation time
ω	angular frequency
$\cdot$	radical

LIST OF FIGURES

LIST OF TABLES

LIST OF APPENDIXES

***Appendix I**: Relative oxo-degradability of individual mulching films under study.*

Mulching film	Photo oxo-degradation in SEPAP 12/24	Thermo oxo-degradation in oven at 60 °C
DCST	3	2
DC89	2	1
DGUV	5	4
10PD	2	5
DCRG	3	2
GDTP	2	3
DC55	1	2
DCN82	4	2

The value 1 stands for the highest oxo-degradability and on the contrary the value 5 means the lowest oxo-degradability.